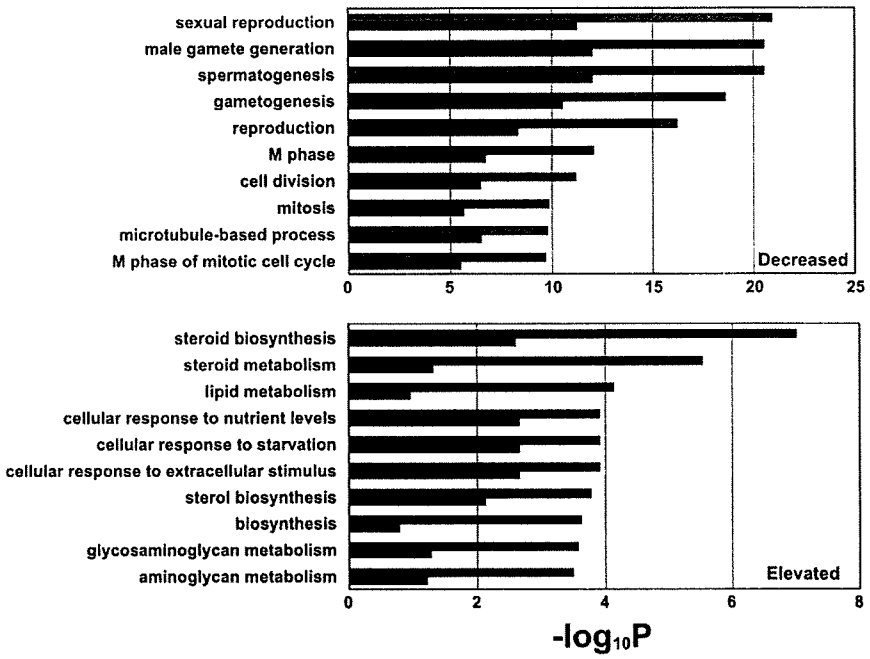

Figure 2. Comparison of Ten Top-ranked Gene Ontology (GO) Categories Significantly Over-Represented in the Two Subsets (1,709 Decreased, Upper Panel; 903 Elevated, Lower Panel) of NOA-related Target Genes

Blue and red bars represent *p*-values for the ten top-ranked GO categories over-represented in the decreased and elevated gene lists, respectively. Black bars show the corresponding *p*-value using 2,611 NOA-related target genes. *p*-Values were determined by Fisher's exact test using all of the GO-annotated genes on the Agilent Human 1A(v2) microarray as a background, as shown in Table 1. The *p*-values are expressed as the negative logarithm (base 10).

doi:10.1371/journal.pgen.0040026.g002

the most reasonable subclassification among 47 NOA samples. For comparative analysis of class discovery, a hierarchical clustering (HC) approach was applied to log-transformed normalized ratios for NOA-related target genes. As shown in Figure 3B, the HC dendrogram exhibited a clustering pattern similar to that of the NMF-based subclassification, as the three NMF-subclasses of NOA samples tended to form distinct clusters in the HC analysis. Thus, the HC clustering for NOA-related target genes appears to justify the three NMF-based subclasses of NOA samples.

To investigate the clinical features of the three NOA subclasses, we compared several clinical measures among the subclasses. The results obtained from statistical analyses in a total of four groups including the OA group are summarized in Table 2. We found significant differences in the three NOA-related clinical characteristics, testicular histological score (Johnsen's score, $p = 1.4 \times 10^{-6}$), serum FSH level ($p = 9.8 \times 10^{-4}$), and LH level ($p = 0.0051$) among the four groups using Kruskal-Wallis test, but there were no differences in age and serum testosterone level. *Post hoc* pairwise comparisons revealed that both the NOA1 and NOA2 groups exhibited low Johnsen's scores and high levels of serum FSH compared with the OA group (Table 2). In the NOA1 group, a high LH level ($p < 0.01$) also was found compared with the OA group. On the other hand, there were no significant differences in any of the parameters between the NOA3 and OA groups, as well as among three NOA subclasses in *post hoc* analysis. Elevations of serum FSH and LH concentrations often are observed in infertile patients with abnormal testicular histologies and are correlated, to some extent, with the severity of spermatogenic defects [9,10]. Testicular histologies of NOA and OA patients have been evaluated by the Johnsen's scores, ranging from 10 to 1 according to the presence or absence of spermatogenesis-related cell types (spermatozoa, spermatids, spermatocytes, spermatogonia, and Sertoli cells) in seminiferous tubules [11]. The NMF-based subclasses of testicular gene expression showed that the low score classes had heterogeneity (NOA1 and NOA2), presumably indicating the possibility of distinct spermatogenic defects at the molecular level that could not be detected by morphological examination.

Identification of Transcripts Differentially Expressed in the Three NOA Subclasses

Based on the three NOA subclasses, we conducted further statistical analyses to extract transcripts representing expression differences between NOA subclasses from the NOA-related target genes (Figure S1). 149 out of 2,611 transcripts showed significant differences ($p < 0.05$, Tukey's *post hoc* test) in testicular expression between the NOA subclasses, as summarized in Table S1. To characterize this gene list based on GO classification for biological processes, we examined which GO terms were highly associated with the 149 differentially expressed transcripts, relative to those for the NOA-related gene list (as shown in Table 1 and Figure 2). Figure 4 shows the 10 top-ranked GO categories for the 149 transcripts, using the 2,611 NOA-related target transcripts as a background set of genes for this GO analysis. Nine GO categories excluding gametogenesis appeared to be novel, indicating that highly significant enrichments of transcripts involved in DNA metabolism (GO:6259; 6325; 6323; 6281),

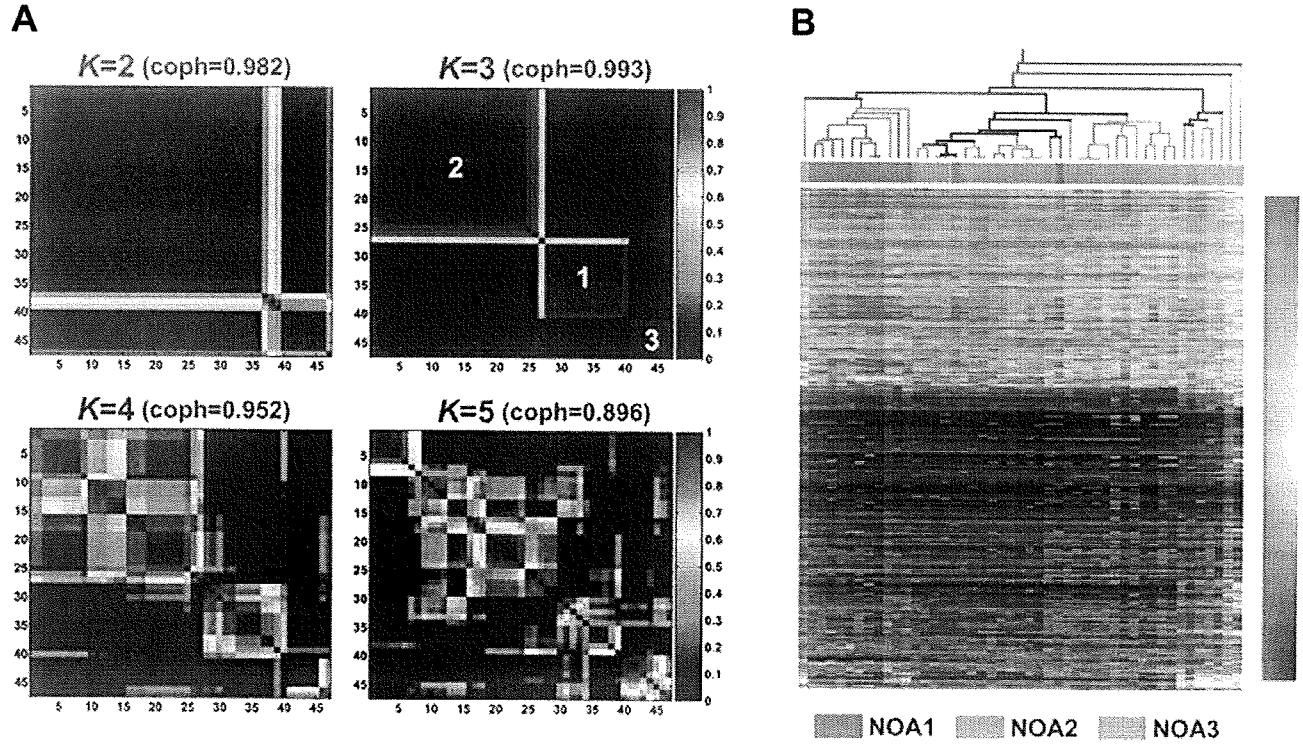

Figure 3. Non-Negative Matrix Factorization (NMF) and Hierarchical Clustering (HC)-based Subclassification of 47 NOA Samples

(A) Reordered consensus matrices averaging 50 connectivity matrices computed at $K = 2$–5 (as the number of subclasses modeled) for the NOA data set comprising of NOA-related target genes. NMF computation and model selection were performed according to Brunet et al. [6] as described in Materials and Methods. According to cophenetic correlation coefficients (coph) for NMF-clustered matrices, the NMF class assignment for $K = 3$ was the most robust.

(B) The HC method incorporated in GeneSpring also was used to classify NOA heterogeneity in testicular gene expression. To display correspondences of subclassification by the two methods, the NMF class assignments for $K = 3$ are shown color-coded; NOA1 (green), NOA2 (pink), and NOA3 (light purple).

doi:10.1371/journal.pgen.0040026.g003

chromosome organization and biogenesis (GO:51276; 7001), sex differentiation (GO: 7548), and response to endogenous stimulus (GO:9719; 6974) occurred after the extraction of 149 transcripts from the NOA-related target gene list (Figure 4). Other features of the 149 transcripts from the gene list (Table S1) were as follows: (1) a high frequency (24.2%) of sex chromosome-linked genes; (2) a high frequency (13.4%) of genes encoding cancer/testis antigens [12,13]; and (3) a moderate frequency (6.7%) of male infertility-related genes. Defect of these genes results in male infertility/subfertility in mice [3,14–16].

Twenty-five of the 149 transcripts showing differences in between-subclass expression displayed elevated expression in NOA, while the others (124 transcripts) had decreased expression (Table S1). The 25 NOA-elevated transcripts accounted only for differences in testicular expression between NOA1 and the other two subclasses, NOA2 and NOA3 (Figure S2; Table S1), suggesting testicular hyperactivity in NOA1 patients. For example, 3β-hydroxysteroid dehydrogenase, encoded by *HSD3B2* and *HSD3B1*, plays a crucial role in biosynthesis of testosterone in Leydig cells [17]. Expression levels of the two transcripts in the NOA1 subclass were higher than those in the NOA2 and NOA3 subclasses, and the expression difference between NOA1 and NOA3 was significant by Tukey's *post hoc* test (Figure S2; Table S1). As the NOA1 subclass showed significantly high LH and slightly low testosterone levels (Table 2), the elevated levels of the two transcripts may be explained by a compensation process for maintaining normal testosterone level. Thus, such enhanced steroidogenesis of the NOA1 subclass might favor, even if only slightly, testicular hyperactivity in NOA1 patients.

On the other hand, among the 124 NOA-decreased transcripts, most transcripts (118/124) showed expression differences between NOA3 and the other two subclasses (Figures S2–S4; Table S1). Expression levels of these transcripts in the NOA3 subclass were similar to those in testis reference RNA (Figures S2–S4), indicating that the NOA3 subclass has a mild defect in spermatogenesis. This notion is supported by the fact that the expression of *INHBB* encoding inhibin β subunit B in the NOA3 subclass is normal while NOA1 and NOA2 subclasses showed low levels, indicating that inhibin β may be a marker of testicular dysfunction, as previously reported [18].

Verification of Between-Subclass Differences in Testicular Expression by Quantitative Real-Time RT-PCR

To evaluate the appropriateness of microarray data on transcripts representing expression differences between NOA subclasses, we selected 53 with high significance ($p < 0.01$, Tukey's *post hoc* test, Figure S1 and Table S1) out of the 149 differentially expressed transcripts and subjected them to real-time RT-PCR analysis. Of the 53 transcripts, the highly

Table 2. Clinical Characteristics of Three Molecular Subclasses of NOA

Group	*n*	Age (Years)	Range	Johnsen's Score*	Range	Serum FSH (mIU/ml)*	Range	Serum LH (mIU/ml)*	Range	Serum T (ng/ml)	Range
OA	11	33.3 ± 8.5	25–57	7.9 ± 1.2	5.1–9	10.1 ± 9.3	3.6–31.4	4.5 ± 2.3	1.3–9.3	4.8 ± 1.7	3.4–7.0
NOA1	13	37.5 ± 6.0	27–52	2.0 ± 1.0[a]	1–4	34.5 ± 11.5[a]	19.0–53.3	13.6 ± 6.0[a]	5.2–20.8	2.8 ± 1.0	1.4–4.7
NOA2	27	34.4 ± 5.6	24–46	2.2 ± 1.1[b]	1–6	28.3 ± 6.4[c]	19.0–39.3	7.2 ± 2.6	2.4–13.0	3.7 ± 1.4	2.2–5.8
NOA3	7	33.0 ± 4.8	26–40	4.0 ± 1.6	2–6.5	22.7 ± 8.8	12.6–28.6	5.9 ± 0.9	5.3–7.0	4.3 ± 2.7	2.0–7.3

The data are represented as mean ± standard deviation.
*$p < 0.01$ (Kruskal-Wallis test between four groups).
[a]$p < 0.01$, NOA1 versus OA (Scheffe's *posthoc* test on Johnsen's score, FSH and LH between four groups).
[b]$p < 0.01$, NOA2 versus OA (Scheffe's *posthoc* test on Johnsen's score, FSH and LH between four groups).
[c]$p < 0.05$, NOA2 versus OA (Scheffe's *posthoc* test on Johnsen's score, FSH and LH between four groups).
FSH, follicle-stimulating hormone; LH, luteinizing hormone; T, testosterone.
doi:10.1371/journal.pgen.0040026.t002

homologous VCX family genes, *VCX*, *VCX2*, and *VCX3A*, were detected with non-specific assay as a mixture of transcripts. Thus, 50 genes and one gene mixture were subjected to real-time RT-PCR. As shown in Figure S5, real-time RT-PCR data of the 51 transcripts were highly correlated with the results of microarray analysis, the squares of correlation coefficients (R^2) ranging from 0.40 (CT45-2) to 0.90 (GAJ). This validation analysis also provided statistically positive evidence on between-subclass differences for all of the 51 transcripts ($p < 0.05$ with Kruskal-Wallis test, data not shown).

Screening of Candidate Genes for Genetic Susceptibility for NOA

One approach to prioritizing candidate genes for genetic susceptibility underlying NOA is to adopt gene expression data from NOA tissues. Genes that show differences in expression level between NOA subclasses regardless of biological impact were selected based on the concept that polymorphic variation in gene expression among unrelated individuals is largely due to polymorphisms in DNA sequence [19,20]. 52 genes having statistical differences in expression ($p < 0.01$, Table S1) were regarded as candidates for allelic association with NOA. Despite the fact that these genes were not selected based on pathological relevance to NOA, genes such as *SYCP3*, *DAZL*, and *INHBB*, which were reported to function in spermatogenesis were included [21–23]. 191 single nucleotide polymorphisms (SNPs) of 42 genes were subjected to allelic association study with 190 NOA patients and 190 fertile men in the first round of screening. Ten genes

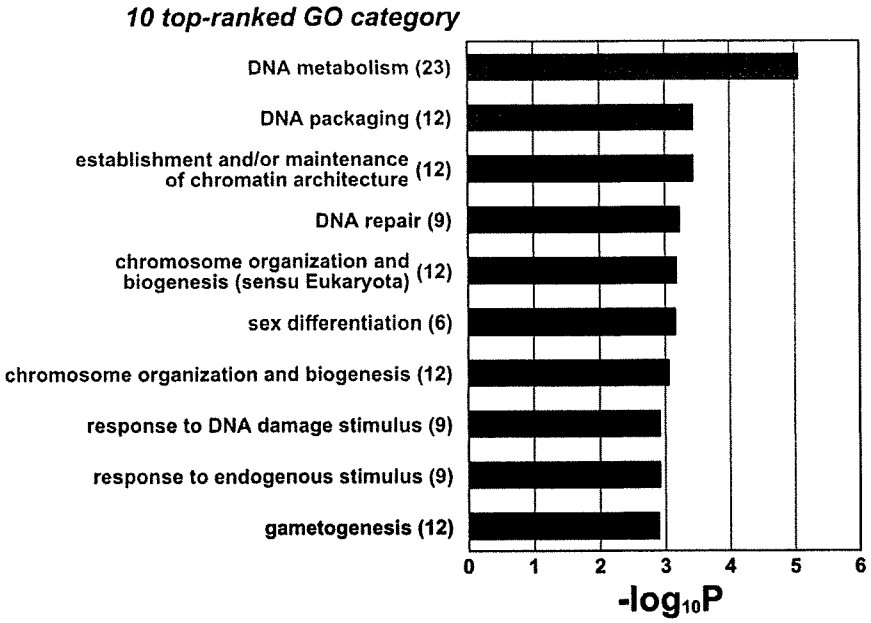

Figure 4. Significant Enrichments of Gene Ontology Categories in GO-based Profiling of 149 Differentially Expressed Transcripts

Grey bars represent *p*-values (expressed as the negative logarithm [base 10]) for the 10 top-ranked GO categories over-represented in the 149 differentially expressed transcripts, using the 2,611 NOA-related target transcripts as a background set of genes for the determination of *p*-values. The actual number of differentially expressed transcripts involved in each category is given in parentheses. In the process of extracting the 149 transcripts from the NOA-related target gene list, sets of genes involved in nine GO categories, marked in magenta, were more condensed because they were not found in the previous 10 top-ranked GO lists of NOA-related target genes (see Table 1 and Figure 2).
doi:10.1371/journal.pgen.0040026.g004

Table 3. Analyses of Allelic Association between 44 SNPs of Seven Candidate Genes and Japanese NOA in Second Round of Initial Screening (380 Cases versus 380 Controls)

Gene	Map	rs ID	Sequence Position[a]	Localization	Variation	MAF		χ^2	Nominal *p*
						Case	Control		
ART3	**4q21.1**	rs9995300	−2520	5′-upstream	A/G	40.7%	34.6%	5.60	0.018
		rs17001357	12048	Intron3	C/T	41.5%	46.4%	3.50	0.061
		rs11097230	19801	Intron3	A/G	32.9%	40.1%	7.79	0.0053
		rs6836703	34283	Intron11	G/A	41.4%	32.8%	11.7	0.00061*
		rs1128864	37726	Exon12-Non-synonymous	T/C	39.3%	33.2%	5.53	0.019
		rs6840007	43329	3′-downstream	A/T	34.5%	28.4%	6.16	0.013
LOC92196	**2q24.1**	rs4254463	−5901	5′-upstream	G/A	18.1%	16.7%	0.46	0.50
		rs908404	2538	Intron1	T/C	17.9%	16.1%	0.69	0.41
		rs9869	11757	Exon3-non-synonymous	C/T	19.7%	14.8%	5.85	0.016
		rs10016	20600	3′-UTR	G/A	9.8%	10.0%	0.00	0.99
NYD-SP20	**17p13.3**	rs3829957	−3785	5′-upstream	C/T	36.0%	36.2%	0.00	0.99
		rs2318035	12022	Intron5	A/G	36.9%	36.1%	0.09	0.77
		rs1488689	22797	Exon6-non-synonymous	A/G	34.8%	34.5%	0.01	0.94
		rs17822627	31572	Exon9-synonymous	T/C	35.6%	34.3%	0.23	0.63
		rs2318033	40646	3′-downstream	A/T	37.3%	36.4%	0.10	0.75
PAGE5	**Xp11.21**	rs2148982	2260	Intron3	G/A	30.9%	30.2%	0.01	0.92
		rs5913800	5332	3′-downstream	A/G	31.0%	29.8%	0.06	0.81
		rs5914276	8924	3′-downstream	C/G	31.4%	29.0%	0.40	0.53
		rs11091394	14424	3′-downstream	A/G	32.4%	28.2%	1.15	0.28
TEX14	**17q22**	rs686425	−7314	5′-upstream	G/A	47.1%	47.3%	0.00	0.99
		rs302874	1420	Intron1	C/T	47.3%	47.2%	0.00	0.99
		rs302865	12439	Intron1	C/T	46.7%	46.3%	0.01	0.93
		rs446613	19870	Intron1	A/C	47.6%	49.1%	0.27	0.60
		rs1631237	34721	Intron2	C/T	46.6%	47.3%	0.05	0.82
		rs302843	41430	Intron2	A/G	46.1%	49.0%	0.87	0.35
		rs2611782	51460	Intron2	C/T	47.5%	47.3%	0.00	0.99
		rs591200	63515	Intron2	C/T	42.8%	41.3%	0.25	0.62
		rs9898626	71197	Intron5	G/C	47.1%	46.4%	0.04	0.85
		rs302854	85804	Intron10	T/C	47.0%	48.0%	0.10	0.75
		rs8072873	100367	Intron15	G/C	24.6%	26.0%	0.30	0.58
		rs6503870	110398	Exon20-non-synonymous	T/C	46.8%	47.0%	0.00	0.95
		rs1267542	114726	Intron22	T/C	45.9%	49.1%	0.94	0.33
		rs3803751	119060	Intron24	T/C	23.5%	25.3%	0.61	0.43
		rs1267545	122507	Intron26	G/A	46.0%	48.1%	0.47	0.49
		rs1974586	128685	Intron29	C/T	23.5%	26.6%	1.67	0.20
		rs2333332	138362	3′-downstream	T/C	48.4%	49.0%	0.04	0.85
		rs714959	140815	3′-downstream	T/C	23.6%	22.6%	0.17	0.68
		rs12453459	145125	3′-downstream	C/T	49.0%	45.6%	0.90	0.34
TKTL1	**Xq28**	rs631	−8147	5′-upstream	G/A	23.4%	18.5%	2.37	0.12
		rs6655282	12986	Intron6	G/A	10.7%	6.8%	3.17	0.075
		rs766420	20834	Intron9	C/G	23.7%	22.7%	0.05	0.82
		rs2872817	24848	3′-UTR	A/G	28.5%	26.8%	0.18	0.67
		rs5945413	30181	3′-downstream	A/T	27.2%	27.0%	0.00	0.99
XAGE5	**Xp11.22**	rs4543711	5279	Intron4	A/G	4.9%	7.9%	2.30	0.13

[a]Nucleotide position from the first nucleotide of exon 1 of each gene.
*Statistically significant (corrected $p = 0.027$) based on Bonferroni-corrected *p*-value.
doi:10.1371/journal.pgen.0040026.t003

(*CTAG1B*, *LOC158812*, *LOC255313*, *MAGEA2*, *PEPP-2*, *TSPY1*, *TSPY2*, *VCX3A*, *VCY*, and *XAGE1*) were not analyzed because no gene-based SNPs with minor allele frequency (MAF) > 0.05 could be found. We identified seven genes (*ART3*, *LOC92196*, *NYD-SP20*, *PAGE5*, *TEX14*, *TKTL1*, and *XAGE5*) with at least one SNP showing a discrepancy in MAF of 5% or greater between cases and controls (Table S2). Forty-four SNPs in the seven genes were subjected to a second round of screening by increasing sample size (380 NOA patients and 380 fertile men). After the two rounds of screenings, only one SNP (rs6836703) of *ART3* (ADP-ribosyltransferase 3) was positively associated with NOA after Bonferroni's correction for multiple testing (Table 3; $\chi^2 = 11.7$, corrected $p = 0.027$).

Allelic Association Study with *ART3*

We focused on *ART3* based on the result of the two rounds of screenings, and identified 38 SNPs with MAF > 0.1 by database search or direct sequencing of the gene. 442 NOA patients (cases) and 475 fertile men (controls) were genotyped. Because we intended in this study to find a common genetic cause for NOA, patients with microdeletions of the Y chromosome at the azoospermia factor (AZF) locus, one of the major causes of NOA [1,2], were not excluded from the cases. However, to characterize the cases in regard to the AZF deletions, we examined the incidence of the deletions in a subset of the cases. Of the 442 NOA patients, 99 were examined by PCR-based screening. Fourteen (14.1 %) of the

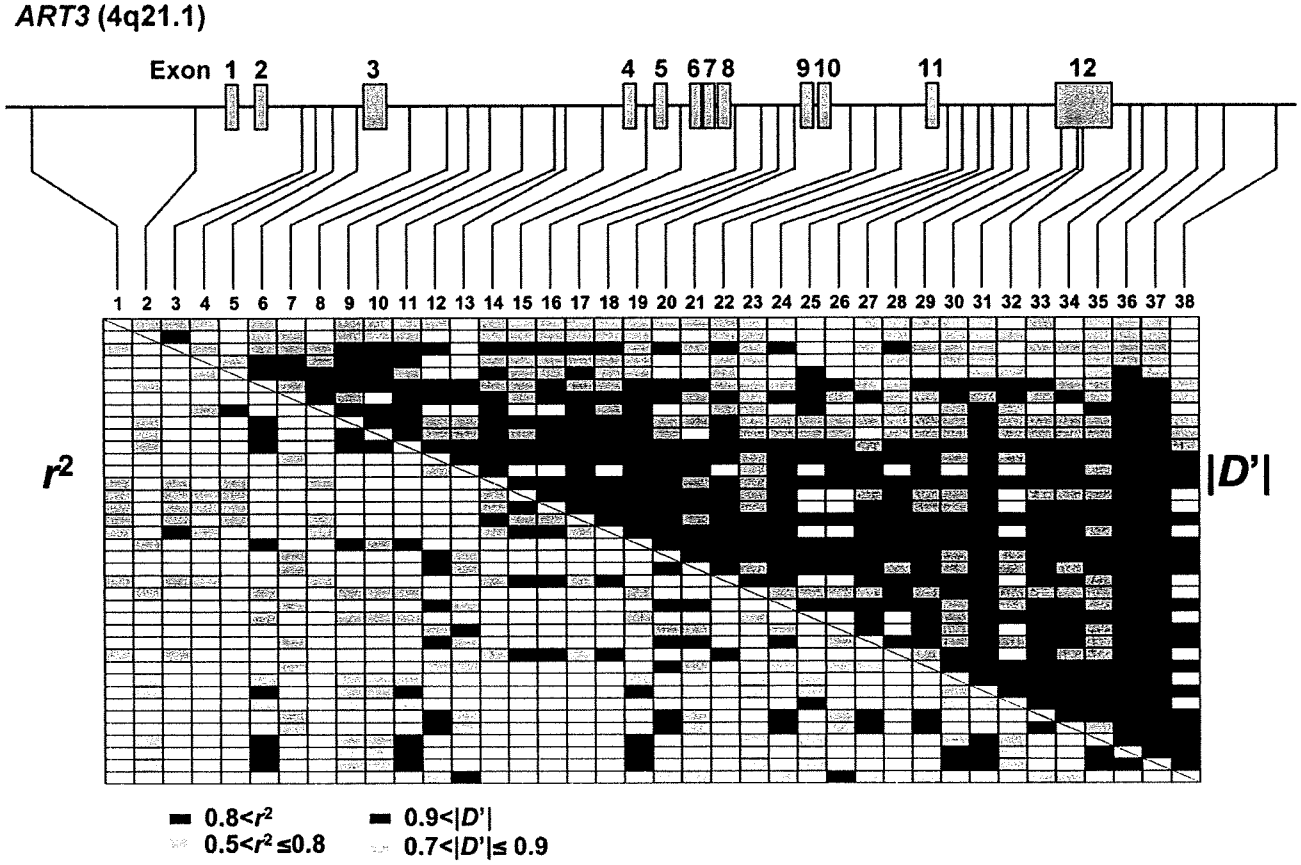

Figure 5. Linkage Disequilibrium Pattern of *ART3*

The gene structure together with the position of 38 SNPs is shown. Pairwise LD coefficients, D' and r^2, of controls were determined and expressed as a block structure. In the schematic block, red boxes indicate pairwise LD of $|D'| > 0.9$ or $r^2 > 0.8$ and pink boxes $0.9 \geq |D'| > 0.7$ or $0.8 \geq r^2 > 0.5$. Blank boxes represent $|D'| \leq 0.7$ or $r^2 \leq 0.5$.

doi:10.1371/journal.pgen.0040026.g005

99 cases examined showed the AZF deletions, and NOA patients with AZFc deletions were most frequent among the 14 cases (data not shown). The overall deletion frequency was comparable to those of other studies [1,2], in which the higher incidence of AZFc deletions also was observed. The clinical characteristics of patients with the AZF deletions did not differ from those of the other NOA patients (data not shown).

Linkage disequilibrium map showed that all of the SNPs of *ART3* were in near complete LD evaluated with D' statistic ($|D'| > 0.7$) in both cases and controls (only controls are displayed in Figure 5). None of the SNPs in the controls showed deviation from Hardy-Weinberg's equilibrium at a threshold of $p < 0.01$ (data not shown). As shown in Table 4, SNPs showing positive associations based on nominal p-values were widely distributed throughout *ART3*. The most significant association was observed with ART3-SNP25 (rs6836703) located in intron 11 of *ART3* ($\chi^2 = 9.16$, nominal $p = 0.0025$, odds ratio [95% CI] = 1.34 [1.11–1.63]). We applied the permutation method for adjustment of multiple testing to avoid a false positive result [24]. A total of four SNPs including ART3-SNP25 met the empirical significance level of $p < 0.05$ (Table 4).

For the haplotype-based association study, we first selected five SNPs (ART3-SNP1, 5, 23, 25, and 28) as tag SNPs captured through LD in *ART3* from 15 SNPs with nominal $p < 0.05$ at a threshold of $r^2 \geq 0.8$ with Tagger software [25]. Haplotype frequencies were inferred using an expectation-maximization (EM) algorithm. After excluding rare haplotypes (frequency < 0.01), association of ART3 haplotypes with NOA was examined in 442 cases and 475 controls. Haplotype H1, the most common haplotype in controls, was under-represented in cases with significance (Figure 6; 26.6% in cases and 35.3 % in controls; $\chi^2 = 15.7$, df = 1, nominal $p = 0.000073$), indicating a protective impact of haplotype H1. After Bonferroni's correction for multiple testing, a protective effect of haplotype H1 was still significant (corrected $p = 0.00080$). Other haplotypes showed no significant difference in frequencies between cases and controls (Figure 6). We also applied a Bayesian algorithm for phasing haplotypes with PHASE version 2.1.1 [26,27]. Regardless of haplotype-phasing methods, haplotype H1 was the most frequent in controls (26.4% in cases and 35.0% in controls), and a significant difference in haplotype H1 frequency between cases and controls was observed (permutation $p < 0.0001$ in global comparison, generated after 10,000 iterations).

Clinical Relevance of the Haplotype Associations

The functional relevance of haplotype H1 in comparison with the clinical data was then explored. Diplotype was

Table 4. Allelic Association of 38 SNPs in *ART3* with NOA in Japanese Population (442 NOA Patients versus 475 Controls)

Number	rs ID	Sequence Position[a]	Localization	Variation	MAF		χ^2	Nominal *p*	Permutation *p*[b]
					Case	Control			
ART3-1	rs13111494	−10376	5′-upstream	T/C	37.7%	43.4%	3.96	0.047	0.36
ART3-2	rs9995300	−2520	5′-upstream	A/G	38.7%	35.8%	1.66	0.20	0.81
ART3-3	rs4859609	3333	intron2	A/G	39.3%	43.2%	2.84	0.092	0.55
ART3-4	rs7666159	3941	intron2	T/C	51.5%	48.7%	1.40	0.24	0.87
ART3-5	rs4859611	5562	intron2	T/C	43.9%	48.8%	4.42	0.035	0.29
ART3-6	rs10007524	7070	intron2	G/A	34.6%	30.7%	3.14	0.077	0.49
ART3-7	rs4859612	9950	intron3	T/G	16.8%	17.8%	0.29	0.59	1
ART3-8	rs17001357	12048	intron3	C/T	40.6%	45.9%	5.13	0.024	0.22
ART3-9	rs4308383	12986	intron3	C/T	35.8%	31.2%	4.24	0.040	0.32
ART3-10	rs17001364	13478	intron3	T/C	36.4%	31.2%	5.47	0.019	0.19
ART3-11	rs7675618	15549	intron3	G/A	35.0%	30.3%	4.33	0.038	0.31
ART3-12	rs4859422	16736	intron3	G/A	23.2%	25.1%	0.88	0.35	0.96
ART3-13	rs4859614	17327	intron3	G/A	32.8%	31.2%	0.51	0.48	1
ART3-14	**rs11097230**	**19801**	**intron3**	**A/G**	**32.5%**	**39.3%**	**8.73**	**0.0031**	**0.040**
ART3-15	rs6829592	23717	intron4	G/A	43.3%	46.0%	1.32	0.25	0.89
ART3-16	rs13131187	25213	intron5	A/G	42.3%	45.1%	1.46	0.23	0.86
ART3-17	**rs17001385**	**26422**	**intron8**	**C/G**	**32.5%**	**39.2%**	**8.84**	**0.0030**	**0.038**
ART3-18	rs12331871	27635	intron8	T/G	39.7%	43.5%	2.57	0.11	0.61
ART3-19	rs17001390	28316	intron8	C/T	34.3%	30.2%	3.49	0.062	0.43
ART3-20	rs12510869	28670	intron8	A/G	23.2%	24.4%	0.36	0.55	1
ART3-21	rs13130116	29976	intron10	C/T	22.6%	24.9%	1.28	0.26	0.90
ART3-22	rs9307076	31256	intron10	G/A	40.3%	43.5%	1.92	0.17	0.75
ART3-23	rs4599438	32278	intron10	A/G	37.5%	31.7%	6.71	0.010	0.11
ART3-24	rs17001409	33549	intron11	T/C	23.8%	25.1%	0.39	0.53	1
ART3-25	**rs6836703**	**34283**	**intron11**	**G/A**	**41.2%**	**34.3%**	**9.16**	**0.0025**	**0.034**
ART3-26	rs4241584	35127	intron11	C/T	30.3%	29.5%	0.13	0.72	1
ART3-27	rs4859423	35158	intron11	T/C	23.7%	25.3%	0.67	0.41	0.99
ART3-28	rs4241586	35506	intron11	T/C	39.7%	44.5%	4.14	0.042	0.33
ART3-29	rs17001416	35935	intron11	G/T	21.6%	22.5%	0.20	0.66	1
ART3-30	rs1128864	37726	exon12-non-synonymous	T/C	38.2%	33.8%	3.72	0.054	0.39
ART3-31	New	37857	exon12-3′-UTR	G/A	34.1%	29.4%	4.58	0.032	0.28
ART3-32	**rs14773**	**37861**	**exon12-3′-UTR**	**A/C**	**45.0%**	**38.1%**	**8.96**	**0.0028**	**0.036**
ART3-33	rs7689378	38491	3′-downstream	A/G	21.7%	23.4%	0.67	0.41	0.99
ART3-34	rs13141802	38730	3′-downstream	G/C	22.3%	24.2%	0.86	0.35	0.97
ART3-35	rs10654	40031	3′-downstream	T/A	34.8%	30.5%	3.64	0.056	0.41
ART3-36	rs7675107	41918	3′-downstream	A/G	33.6%	29.1%	4.19	0.041	0.32
ART3-37	rs6840007	43329	3′-downstream	A/T	34.3%	29.7%	4.42	0.036	0.30
ART3-38	rs4538520	49092	3′-downstream	C/T	33.1%	31.7%	0.39	0.53	1

SNPs in bold show statistical significance and are subjected to haplotype analysis as shown in Figure 6.
[a]Nucleotide position from the first nucleotide of exon 1.
[b]Permutation *p*-values generated by 10,000 iterations. SNPs in bold show statistical significance based on the permutation *p*-values.
doi:10.1371/journal.pgen.0040026.t004

inferred with EM algorithm, and three categories (code 0, 1, and 2) were defined by the number of haplotype H1 carried without counting the other haplotypes, and nonparametric analysis of variance test with clinical data was performed. Serum levels of hormones (LH, FSH, and testosterone), other biochemical and pathophysiological markers, and Johnsen's score were analyzed by Kruskal-Wallis test with a Bonferroni/Dunn *post hoc* test between the three diplogroups. Serum testosterone levels were significantly different among the three groups (Figure 7; df = 2, $p = 0.0093$), but there were no significant differences in other clinical markers. *Post hoc* pairwise comparisons revealed that serum testosterone levels were significantly higher in the subgroup having two copies of haplotype H1 than in a subgroup with one or no haplotype H1 ($p = 0.0064$ or $p = 0.0004$, respectively, Figure 7). PHASE-inferred individual diplotypes also revealed a similar correlation between diplogroups of haplotype H1 and serum testosterone levels (data not shown).

ART3 Protein Localization in Azoospermic Testis

ART3 protein expression in azoospermic testes was examined by immunohistochemical analysis. As shown in Figure 8, specific staining of ART3 protein was predominantly observed in spermatocytes in OA testes (Figure 8C–8E) as well as in normal testes from individuals of accidental sudden-death (Figure 8A and 8B). Staining was not observed in other stages of undifferentiated germ cells or Sertoli cells in the seminiferous tubules, or the interstitial tissues such as Leydig cells. On the other hand, we did not detect any ART3 protein in NOA testes with Johnsen's scores ranging from 2 to 3, which showed no spermatocytes, spermatids, or spermatozoa in the seminiferous tubules ($n = 12$ samples; Figure 8F–8H). There was no marked difference in testicular ART3

Haplotype	ART3-SNP#					Freq (EM)		χ^2	*P*-value
	1	5	23	25	28	Control	NOA		
H1	C	C	A	G	C	35.3%	26.6%	15.7	0.000073
H2	T	T	G	A	T	27.5%	28.5%	0.21	0.65
H3	T	T	A	G	T	13.8%	13.4%	0.04	0.84
H4	T	C	A	G	T	7.2%	6.4%	0.47	0.50
H5	C	T	A	A	C	3.0%	4.6%	3.10	0.078
H6	T	C	A	G	C	2.6%	3.2%	0.42	0.52
H7	T	C	G	G	T	1.7%	3.0%	3.22	0.07
H8	C	T	A	G	T	2.0%	1.7%	0.16	0.69
H9	T	T	A	A	C	1.2%	1.7%	0.87	0.35
H10	T	T	A	G	C	1.5%	1.0%	0.62	0.43
Others						4.2%	9.9%		

Figure 6. Haplotype-based Association Study of *ART3*

The expectation-maximization (EM) algorithm [37] was used to infer *ART3* haplotype frequencies with genotyping data of five tag SNPs, ART3-SNP1, 5, 8, 23, 25, and 28 (see Table 4). At the respective SNP sites, red and blue boxes represent minor and major alleles, respectively.

doi:10.1371/journal.pgen.0040026.g006

protein expression among the three *ART3* diplo-groups carrying none, one, or two copies of haplotype H1.

Discussion

Genomic Analysis of NOA

Our investigation was designed to clarify the pathogenesis of NOA using global gene expression analyses of testis samples from NOA patients and to identify genetic susceptibilities underlying NOA from the genes differentially expressed. Large families with multiple generations having NOA cannot be expected due to the nature of infertility, so linkage study is impractical for NOA and has not been reported. Alternatively, allelic association study is a practical approach to identification of genetic susceptibility underlying NOA. Thus far, more than 80 genes have been identified as essential for male infertility in humans and mice [3]. Genes on the Y chromosome were emphasized because of observed microdeletions in patients, and genes such as DAZ and HSFY were examined for possible susceptibility genes [28,29]. Recently, homozygous mutation of the aurora kinase C gene was identified in large-headed multiflagellar polyploid spermatozoa, a rare form of infertility, using homozygosity mapping [30]. In the current study, we applied a novel approach to identify common susceptibility genes for NOA by applying global gene expression analysis of NOA testes. Based on the hypothesis that a common variant of a susceptibility gene has resulted in altered expression in tissues relevant to disease etiology [31], we first elucidated the gene expression profile in testes of NOA patients and characterized the genetic pathways that were either under-expressed or over-expressed. Because spermatogenesis is a complex differentiation process, NOA could result from a defect at any stage of the process. Thus, gene expression profiling of NOA tissues might well be confounded by the difficulty of discerning the differential stage and the pathological status. Feig et al. [4] examined stage-specific gene expression profiles in human NOA patients after classification on the basis of Johnsen's score. The testis tissues were classified into four groups showing Sertoli-cell only syndrome, meiotic arrest, testicular hypospermia, and testicular normospermia, corresponding to Johnsen's score 2, 5, 8, and 10, respectively, and stage-specific differential gene expression was monitored. We sought to identify susceptibility genes underlying NOA that could affect any stage of spermatogenesis. Testis samples subgrouped according to Johnsen's score in advance might identify genes affecting multiple stages of spermatogenesis. Therefore, we globally subgrouped the samples at diverse stages of differentiation using an NMF method for reducing multidimensionality that is appropriate for application to high dimensional biological data. The NMF method subgrouped three classes, NOA1, NOA2, and NOA3, which also were unequivocally subgrouped by the HC approach (Figure 3). Notably, NOA1 and NOA2 represent a pathologically similar type showing low Johnsen's score, but were subclassified because of their distinct gene expression pattern. NOA1 and NOA2 showed differences in LH, FSH, and testosterone levels, thus establishing meaningful biological significance of the sub-classes (Table 2).

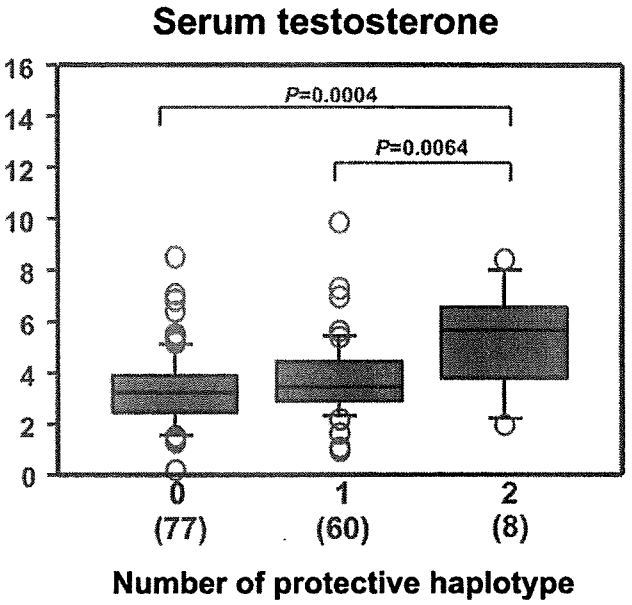

Figure 7. Diplotype-Specific Differences in Serum Testosterone Levels in NOA Patients

Three diplo-groups (code 0, 1, and 2) were defined by the number of *ART3* haplotype H1 carried. The serum testosterone levels were significantly different among the three groups (Kruskal-Wallis; df = 2, $p = 0.0093$) by Bonferroni/Dunn *post hoc* test.

doi:10.1371/journal.pgen.0040026.g007

Genetic Susceptibility to NOA

In the current study, we adopted a novel approach to select candidate susceptibility genes for NOA. Global gene expression analyses were performed on NOA testes, and 52 genes were selected according to differential gene expression between NOA subclasses with a strict statistical criterion ($p < 0.01$ with Tukey's *post hoc* test). Despite the fact that our selection criteria relied only on data regarding differences in gene expression and did not include any biological assumptions, many of the genes were related to spermatogenesis based on Gene Ontology analyses (Figure 4; Table 1). 191 SNPs of 42 genes were screened, and only one gene, *ART3*, showed a positive association after the two rounds of screening. Multiple SNPs of *ART3* were significantly associ-

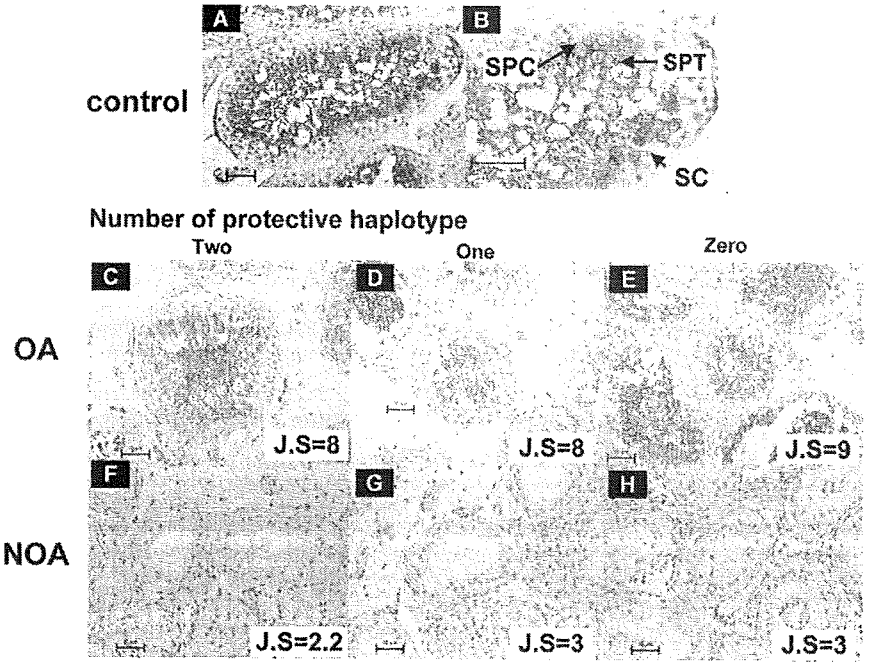

Figure 8. Immunohistochemical Analysis of ART3 Expression in Human Testes

Representative seminiferous tubules in testicular sections from normal controls (A, B), OA (C–E), and NOA patients (F–H) are shown. Arrows indicate spermatocytes (SPC); spermatids (SPT); and Sertoli cells (SC) (B). ART3 protein was immunostained with anti-ART3 antibody; ART3-positive spermatocytes (SPC) are noted as brown staining cells (A–E). No marked differences in testicular ART3 expression among the three ART3 diplo-groups carrying none, one, or two copies of the protective haplotype H1were observed in OA (C–E) and NOA (F–H) patients. Magnification is 60× except in (B) (120×).

doi:10.1371/journal.pgen.0040026.g008

ated with NOA, the most significant association being observed with ART3-SNP25 (rs6836703, nominal $p = 0.0025$, permutation $p = 0.034$; Table 4). We also detected a protective haplotype, H1, which was the most common form and was strongly associated with NOA (nominal $p = 0.000073$, corrected $p = 0.00080$, Figure 6). In addition, diplotype analysis showed that individuals carrying at least one haplotype H1 showed an elevated plasma testosterone level (Figure 7).

Functional Relevance of ART3 in the Pathogenesis of NOA

ART3 is a member of the mono-ADP-ribosyltransferase family genes. The biological function of ART3 remains obscure, as ART3 does not display any detectable arginine-specific transferase activity due to lack of the active site motif (R-S-EXE) that is essential for catalytic activity. Since differentiation of stage-specific expression of ART3 in testis has been reported, protein expression being exclusively present in spermatocytes but absent in spermatozoa [32], a genetic variation of *ART3* might well lead to a functional defect in the process of spermatogenesis. Haplotype H1 of *ART3*, comprising all of the disease-protective alleles at the respective SNP sites, was under-represented in the patients. However, functional disturbance associated with haplotype H1 is so far undetermined despite the fact that several experiments designed to demonstrate haplotype-specific differences in expression level have been performed. Thus, it is possible that this haplotype represents fine tuning that maintains normal maturation of spermatocytes and improves the efficiency of spermatogenesis.

In conclusion, genome-wide gene expression analyses identified differentially expressed genes of NOA subclasses, and *ART3* was identified as a susceptibility gene underlying NOA. This genetic study constitutes only first-stage evidence of association because only Japanese individuals were included, so further replication in independent case-control samples is required to confirm the role of the *ART3* haplotype in genetic risk for NOA. Although further functional evidence is also required, these results provide insight into the pathoetiology of NOA as well as reproductive fitness at the molecular level, and suggest a target for therapy.

Materials and Methods

Participants. Testicular biopsy specimens for microarray analysis were obtained from 47 Japanese patients (aged from 24 to 52 years) with NOA and 11 (aged from 22 to 57 years) with OA, each of whom also underwent testicular sperm extraction (TESE) for assisted reproduction and/or diagnostic biopsy for histological examination. The biopsies for microarray analysis and histological examination were mainly sampled from unilateral, multiple testicular sites in the respective patients. Each patient was first assigned to azoospermia by showing no ejaculated spermatozoa in a semen examination. Subsequently, OA was defined as follows: (1) motile spermatozoa were sampled from microsurgical epididymal sperm aspiration (MESA), or (2) a considerable number of mature spermatozoa was sampled from TESE. NOA was tentatively defined as having no epididymal and/or testicular spermatozoa. The degree of spermatogenic defect was histologically evaluated according to Johnsen's score [11]. At least three biopsies from the same individual were taken, and the average Johnsen's scores in the NOA and OA groups ranged from 1 to 6.5 and from 5.1 to 9, respectively. In most patients, preoperative levels of serum follicle-stimulating hormone (FSH), leutenizing hormone (LH), and total testosterone were measured. The infertile male patients who visited Niigata University, Tachikawa Hospital, and St. Mother's Hospital received a routine semen examination according to 1999 WHO criteria. Based on this analysis, sperm were counted

and the patients who had no ejaculated sperms were enrolled for a case-control association study. In total, 442 patients were ascertained to have NOA. In the current study, azoospermia patients with varicocele, ejaculatory dysfunction, endocrinopathy, or histologically examined OA as defined above were excluded. 475 fertile men having no specific clinical record were recruited in Niigata University. The ethics committees of Niigata University, Tachikawa Hospital, St. Mother's Hospital, and Tokai University approved the study protocols, and each participant gave written informed consent. Genomic DNA was prepared from blood white cells by Dneasy (Qiagen, Tokyo, Japan) or salivas by phenol/chloroform extraction.

To examine microdeletion of the Y chromosome in a subset of NOA patients, PCR-based diagnostic technique was used as follows: PCR amplifications with fluorescence (FAM or HEX)-labeled primers were performed to obtain fragments encompassing each of 13 STS markers in and around azoospermia factor (AZF) regions of the Y chromosome (in AZFa: SY83, SY95 and SY105; in AZFb: SY118, G65320, SY126 and SY136; in AZFc: SY148, SY149, SY152, SY283 and SY1291; in the heterochromatin distal to AZFc: SY166). Primer sequences and PCR conditions are available from the authors on request. PCR-amplified fragments were run on the ABI PRISM 3100 Genetic Analyzer (Applied Biosystems, Tokyo, Japan), and Y-chromosome microdeletion was determined with GENESCAN software (Applied Biosystems).

Microarray analysis of testis samples. Total RNA from testicular biopsy was extracted using TRIzol reagent (Invitrogen, Carlsbad, CA, USA) and quantity and quality of the extracted RNA were examined with 2100 Bioanalyzer (Agilent Technologies, Palo Alto, CA, USA) using RNA 6000 Nano LabChip (Agilent Technologies). Human Testis Total RNA (BD Biosciences, San Jose, CA, USA), a histologically normal testicular RNA pooled from 39 Caucasians, was used as a common reference in two-color microarray experiments.

For fluorescent cRNA synthesis, high-quality total RNA (150 ng) was labeled with the Low RNA Input Fluorescent Linear Amplification Kit (Agilent Technologies) according to the manufacturer's instructions. In this procedure, cyanine 5-CTP (Cy5) and cyanine 3-CTP (Cy3) (PerkinElmer, Boston, MA, USA) were used to generate labeled cRNA from the extracted patient RNA and the reference RNA, respectively. Labeled cRNAs (0.75 μg each) from one patient and the common reference were combined and fragmented in a hybridization mixture with the *In Situ* Hybridization Kit Plus (Agilent Technologies). The mixture was hybridized for 17 hours at 65°C to the Agilent Human 1A(v2) Oligo Microarray, which carries 60-mer probes to 18,716 human transcripts. After hybridization, the microarray was washed with SSC buffer, and then scanned in Cy3 and Cy5 channels with the Agilent DNA Microarray Scanner model G2565AA (Agilent Technologies). Signal intensity per spot was generated from the scanned image with Feature Extraction Software ver7.5 (Agilent Technologies) in default setting. Spots that did not pass quality control procedures were flagged and removed for further analysis.

The Lowess (locally weighted linear regression curve fit) method was applied to normalize the ratio (Cy5/Cy3) of the signal intensities generated in each microarray with GeneSpring GX 7.3 (Agilent Technologies). Compared with the expression level of reference RNA, the NOA group, with expression undergoing a 2-fold mean change or more was extracted; the OA group comprised transcripts showing less than 2-fold mean expression change (Figure 1A). Of the transcripts included in both groups, only those with a statistically significant difference in expression between NOA and OA testes (based on lowess-normalized natural log[Cy5/Cy3], Bonferroni's corrected $p < 0.05$) were counted as NOA-related target genes. To elucidate the molecular subtypes of NOA, we adopted the non-negative matrix factorization (NMF) algorithm, which has been recently introduced to analysis of gene expression data [5,6]. For this analysis, a complete dataset without missing values was generated from raw values of Cy5 intensities for the NOA-related target genes in the NOA samples, and used to clarify NOA heterogeneity using three M-files (available from the following URL; http://www.broad.mit.edu/cgi-bin/cancer/publications/pub_paper.cgi?mode=view&paper_id=89) for MATLAB (Mathworks, Natick, MA, USA). According to the subclassification of NOA samples, transcripts differentially expressed between NOA subclasses were determined by one-way ANOVA, followed by Tukey's *post hoc* test in GeneSpring GX. For multiple test corrections in this statistical analysis, we used the Benjamini-Hochberg procedure [33] of controlling the false discovery rate (FDR) at the level of 0.05 or 0.01. To analyze which categories of Gene Ontology were statistically overrepresented among the gene lists obtained, we used GO Browser, an optional tool in GeneSpring GX, where the statistical significance was determined by Fisher's exact test. The microarray data reported in this paper have been deposited in the Gene Expression Omnibus (GEO, http://www.ncbi.nlm.nih.gov/geo/) database, and are accessible through GEO Series accession number GSE9210.

Quantitative real-time RT-PCR analysis for validation of between-subclass differences in gene expression. Quantitative real-time RT-PCR analysis was used to verify the microarray data on 53 transcripts representing differential expressions between NOA subclasses with high significance ($p < 0.01$). Among 53 transcripts, VCX (NM_013452), VCX2 (NM_016378), and VCX3A (NM_016379) were examined as a single transcript because sequence homologies between the three transcripts prevented development of appropriate assays for discrimination. Testicular total RNA (1 μg) subjected to microarray analysis was used as a template in first-strand cDNA synthesis with SuperScript III First-Strand Synthesis System (Invitrogen). Each single-stranded cDNA was diluted one-tenth for a subsequent real-time RT-PCR using SYBR *Premix Ex Taq* (Perfect Real Time) (TAKARA BIO, Otsu, Japan) on the ABI PRISM 7900HT Sequence Detection System (Applied Biosystems) according to the manufacturer's instructions. The PCR primers for 43 transcripts showing between-subclass differences with high significance and *GAPDH* were designed and synthesized by TAKARA BIO Inc., or QIAGEN GmbH (as the QuantiTect Primer Assay). In the real-time RT-PCR analysis for the nine remaining transcripts, we used TaqMan Gene Expression Assays (Applied Biosystems) with TaqMan Universal PCR Master Mix (No AmpErase UNG version) according to the manufacturer's instructions (Applied Biosystems). The detailed information on the primer sequences used and/or the assay system selected are summarized in Table S3. A relative quantification method [34] was used to measure the amounts of the respective genes in NOA testes, normalized to *GAPDH* as an endogenous control, and relative to Human Testis Total RNA (BD Biosciences) as a reference RNA. Statistical significance between NOA subclasses was determined by Kruskal-Wallis test, followed by multiple comparisons; $p < 0.05$ was considered significant.

SNP selection of candidate genes for NOA and genotyping. Based on gene expression data of NOA testes, we selected 52 genes (encoding 53 transcripts) as candidates for genetic susceptibilities underlying NOA. SNPs of the candidate genes with minor allele frequency (MAF) > 0.05 were obtained from the NCBI dbSNP database (http://www.ncbi.nlm.nih.gov/SNP/), and applied to an initial screening. Of the 52 candidate genes, 10 genes (CTAG1B, LOC158812, LOC255313, MAGEA2, PEPP-2, TSPY1, TSPY2, VCX3A, VCY, and XAGE1) were excluded from the initial screening because gene-based SNPs with MAF > 0.05 were not found in the public SNP database. A total of 191 SNPs of 42 genes were genotyped in the screening with TaqMan SNP Genotyping Assays on the ABI PRISM 7900HT Sequence Detection System (Applied Biosystems). 190 NOA patients (cases) and 190 fertile men (controls) were genotyped in the first round screening. For genes with at least one SNP showing a discrepancy in MAF of 5% or greater between cases and controls, the sample size was increased to 380 cases and 380 controls in the second round.

After two rounds of initial screening, additional SNPs of *ART3* were selected from dbSNP or identified by direct sequencing of all 12 exons of the gene (Ensemble transcript ID ENST00000355810) and splice acceptor and donor sites in the intron using the genomic DNAs from 95 infertile patients as PCR templates. A total of 38 SNPs of *ART3* were finally genotyped on 442 cases and 475 controls by TaqMan SNP Genotyping Assays or by direct sequencing with BigDye Terminators v3.1 Cycle Sequencing Kit (Applied Biosystems) on ABI PRISM 3700 DNA analyzer.

Statistical analyses in association study. Pairwise linkage disequilibrium (LD), using the standard definition of D' and r^2 [35,36], was measured with SNPAlyze v5.0 software (DYNACOM, Mobara, Japan). To construct *ART3* haplotypes in phase-unknown samples, tag SNPs of *ART3* were selected with Tagger software [25], incorporated in the Haploview. The expectation-maximization (EM) algorithm [37] and PHASE version 2.1.1 [26,27] was used to infer haplotype frequencies and individual diplotypes for *ART3*. Differences in allelic and haplotype frequencies were evaluated using a case-control design with the chi-square test. For an adjustment of multiple testing, we applied a permutation method with Haploview version 3.32 software, or Bonferroni's method to determine corrected p-values.

To investigate association of the *ART3* diplotype with clinical phenotypes such as serum hormone levels, differences among the three categories (code 0, 1, and 2), defined by the number of the most significant haplotype, were statistically examined by Kruskal-Wallis test, followed by Bonferroni/Dunn *post hoc* test (StatView version 5.0, SAS Institute, Cary, NC, USA).

Immunohistochemistry. To examine cellular localization of ART3

protein in azoospermic testes, testicular biopsy specimens from 15 OA and 12 NOA patients were subjected to immunohistochemistry. Four postmortem testicular tissues of accidental sudden-deaths were used as normal controls. The testicular tissues were fixed in 10% buffered formalin and embedded in paraffin. Cryosections (3 μm thickness) were pre-incubated with the Histofine Antigen-Retrieval Solution (1:10 dilution; Nichirei Bioscience, Tokyo, Japan) for 10 minutes at 95 °C. The sections were then incubated with primary ART3 antibody (1:4,000; Abnova, Taipei, Taiwan), then with IgG2b isotype (1:4,000; MBL International, Woburn, USA) for 60 minutes at room temperature. After washing with PBS, the sections were incubated with the Histofine Simple Stain Max-PO (Multi) (1:5 dilution; Nichirei Bioscience) for 30 minutes at room temperature, and then reacted with DAB (Nichirei Bioscience) for 10 minutes at room temperature. Haematoxylin was used for counterstaining.

Supporting Information

Figure S1. Statistical Analysis Reveals Transcripts Differentially Expressed among Three NOA Subclasses

Venn diagram summaries show the number of transcripts differentially expressed with significance by Tukey's *post hoc* test in each comparison (see Table S1)

Found at doi:10.1371/journal.pgen.0040026.sg001 (694 KB EPS).

Figure S2. Comparisons of Expression Levels of 149 Transcripts Expressed Differentially between Three NOA Subclasses in Microarray Analysis (Part I)

Natural log-transformed normalized ratios of NOA to testis reference (*y*-axes) were subjected to statistical analysis, as described in Materials and Methods. Each column represents mean ± standard error of the mean. The 53 transcripts with highly significant ($p < 0.01$, Tukey test) differences between the three NOA subclasses are shown in red.

Found at doi:10.1371/journal.pgen.0040026.sg002 (773 KB EPS).

Figure S3. Comparisons of Expression Levels of 149 Transcripts Expressed Differentially between Three NOA Subclasses in Microarray Analysis (Part II)

Natural log-transformed normalized ratios of NOA to testis reference (*y*-axes) were subjected to statistical analysis, as described in Materials and Methods. Each column represents mean ± standard error of the mean. The 53 transcripts with highly significant ($p < 0.01$, Tukey test) differences between the three NOA subclasses are shown in red.

Found at doi:10.1371/journal.pgen.0040026.sg003 (798 KB EPS).

Figure S4. Comparisons of Expression Levels of 149 Transcripts Expressed Differentially between Three NOA Subclasses in Microarray Analysis (Part III)

Natural log-transformed normalized ratios of NOA to testis reference (*y*-axes) were subjected to statistical analysis, as described in Materials and Methods. Each column represents mean ± standard error of the mean. The 53 transcripts with highly significant ($p < 0.01$, Tukey test) differences between the three NOA subclasses are shown in red.

Found at doi:10.1371/journal.pgen.0040026.sg004 (822 KB EPS).

Figure S5. Correlations of Testicular Gene Expression Evaluated by Microarray and Quantitative Real-Time RT-PCR Analyses

Expression levels of 51 transcripts with highly significant ($p < 0.01$) differences in expression among the three NOA subclasses were quantified by real-time RT-PCR method as described in Material and Methods. Squares of correlation coefficients (R^2) for the respective transcripts were calculated between normalized expression ratios of NOA to testis reference in microarray data (*x*-axes) and the corresponding ratios obtained by real-time RT-PCR analysis (*y*-axes)

Found at doi:10.1371/journal.pgen.0040026.sg005 (1.7 MB EPS).

Table S1. 149 Transcripts Representing Statistically Significant ($p < 0.05$) Differences in Testicular Expression between Three NOA Subclasses

Found at doi:10.1371/journal.pgen.0040026.st001 (68 KB XLS).

Table S2. Comparison of Minor Allele Frequencies (MAFs) at 191 SNPs of 42 Genes between 190 Infertile Patients and 190 Fertile Males (First Round of Initial Screening)

Found at doi:10.1371/journal.pgen.0040026.st002 (415 KB DOC).

Table S3. Quantitative Real-time RT-PCR Assays for 51 Transcripts Representing Highly Significant Differences between NOA Subclasses

Found at doi:10.1371/journal.pgen.0040026.sg003 (30 KB XLS).

Acknowledgments

We thank tissue and DNA donors and supporting medical staff for making this study possible. We are grateful to M. Takamiya, Y. Sakamoto, and K. Otaka for their technical assistance.

Author contributions. AT, KT, and II conceived and designed the experiments. HO and AT performed the experiments and analyzed the data. AT, KS, KT, and II contributed reagents/materials/analysis tools. HO, AT, and II wrote the manuscript. All authors contributed to editing the manuscript. HO and AT have joint authorship of this manuscript.

Funding. This work was supported in part by a Grant-in-Aid for scientific research from the Japanese Ministry of Education, Science, Sports, and Culture; a Grant-in-Aid for the Promotive Operations of Scientific Research on Children and Families from the Japanese Ministry of Health, Labor and Welfare; and 2007 Tokai University School of Medicine Research Aid.

Competing interests. The authors have declared that no competing interests exist.

References

1. Pryor JL, Kent-First M, Muallem A, Van Bergen AH, Nolten W, et al. (1997) Microdeletions in the Y chromosome of infertile men. N Eng J Med 336: 534–539.
2. Krausz C, Rajpert-de Meyts E, Frydelund-Larsen L, Quintana-Murci L, McElreavey K, et al. (2001) Double-blind Y chromosome microdeletion analysis in men with known sperm parameters and reproductive hormone profiles: microdeletions are specific for spermatogenic failure. J Clin Endocrinol Metab 86: 2638–2642.
3. Matzuk MM, Lamb DJ (2002) Genetic dissection of mammalian fertility pathways. Nat Cell Biol 4 (Supplement): S41–S49.
4. Feig C, Kirchhoff C, Ivell R, Naether O, Schulze W, et al. (2006) A new paradigm for profiling testicular gene expression during normal and disturbed human spermatogenesis. Mol Hum Reprod 13: 33–43.
5. Kim PM, Tidor B (2003) Subsystem identification through dimensionality reduction of large-scale gene expression data. Genome Res 13: 1706–1718.
6. Brunet JP, Tamayo P, Golub TR, Mesirov JP (2004) Metagenes and molecular pattern discovery using matrix factorization. Proc Natl Acad Sci U S A 101: 4164–4169.
7. Pascual-Montano A, Carmona-Saez P, Chagoyen M, Tirado F, Carazo JM, et al. (2006) bioNMF: a versatile tool for non-negative matrix factorization in biology. BMC Bioinformatics 7: 366.
8. Churchill GA (2002) Fundamentals of experimental design for cDNA microarrays. Nat Genet 32 (Supplement): 490–495.
9. Micic S (1983) The effect of the gametogenesis on serum FSH, LH and prolactin levels in infertile men. Acta Eur Fertil 14: 337–340.
10. Yaman O, Ozdiler E, Seckiner I, Gogus O (1999) Significance of serum FSH levels and testicular morphology in infertile males. Int Urol Nephrol 31: 519–523.
11. Johnsen SG (1970) Testicular biopsy score count—a method for registration of spermatogenesis in human testes: normal values and results in 335 hypogonadal males. Hormones 1: 2–25.
12. Scanlan MJ, Simpson AJ, Old LJ (2004) The cancer/testis genes: review, standardization, and commentary. Cancer Immun 4: 1.
13. Simpson AJ, Caballero OL, Jungbluth A, Chen YT, Old LJ (2005) Cancer/testis antigens, gametogenesis and cancer. Nat Rev Cancer 5: 615–625.
14. Crackower MA, Kolas NK, Noguchi J, Sarao R, Kikuchi K, et al. (2003) Essential role of Fkbp6 in male fertility and homologous chromosome pairing in meiosis. Science 300: 1291–1295.
15. Spruck CH, de Miguel MP, Smith AP, Ryan A, Stein P, et al. (2003) Requirement of Cks2 for the first metaphase/anaphase transition of mammalian meiosis. Science 300: 647–650.
16. Greenbaum MP, Yan W, Wu MH, Lin YN, Agno JE, et al. (2006) TEX14 is essential for intercellular bridges and fertility in male mice. Proc Natl Acad Sci U S A 103: 4982–4987.
17. Hedger MP, de Kretser DM (2000) Leydig cell function and its regulation. In: McElreavey K, editor. The genetic basis of male infertility. Berlin and Heidelberg: Springer-Verlag. pp. 69–110.
18. Nagata Y, Fujita K, Banzai J, Kojima Y, Kasima K, et al. (2005) Seminal plasma inhibin-B level is a useful predictor of the success of conventional testicular sperm extraction in patients with non-obstructive azoospermia. J Obstet Gynaecol Res 31: 384–388.
19. Cheung VG, Conlin LK, Weber TM, Arcaro M, Jen KY, et al. (2002) Natural

variation in human gene expression assessed in lymphoblastiod cells. Nat Genet 33: 422–425.
20. Morley M, Molony CM, Weber TM, Devlin JL, Ewens KG, et al. (2004) Genetic analysis of genome-wide variation in human gene expression. Nature 430: 743–747.
21. Miyamoto T, Hasuike S, Yogev L, Maduro MR, Ishikawa M, et al. (2003) Azoospermia in patients heterozygous for a mutation in SYCP3. Lancet 362: 1714–1719.
22. Kuo PL, Wang ST, Lin YM, Lin YH, Teng YN, et al. (2004) Expression profiles of the DAZ gene family in human testis with and without spermatogenic failure. Fertil Steril 81: 1034–1040.
23. Marchetti C, Hamdane M, Mitchell V, Mayo K, Devisme L, et al. (2003) Immunolocalization of inhibin and activin alpha and betaB subunits and expression of corresponding messenger RNAs in the human adult testis. Biol Reprod 68: 230–235.
24. Churchill GA, Doerge RW (1997) Empirical threshold values for quantitative trait mapping. Genetics 138: 963–971.
25. de Bakker PI, Yelensky R, Pe'er I, Gabriel SB, Daly MJ, et al. (2005) Efficiency and power in genetic association studies. Nat Genet 37: 1217–1223.
26. Stephens M, Smith NJ, Donnelly P (2001) A new statistical method for haplotype reconstruction from population data. Am J Hum Genet 68: 978–989.
27. Stephens M, Donnelly P (2003) A comparison of Bayesian methods for haplotype reconstruction from population genotype data. Am J Hum Genet 73: 1162–1169.
28. Szmulewicz M, Ruiz LM, Reategui EP, Hussini S, Herrera RJ (2002) Single-nucleotide variant in multiple copies of a deleted in azoospermia (DAZ) sequence—a human Y chromosome quantitative polymorphism. Hum Hered 53: 8–17.
29. Vinci G, Raicu F, Popa L, Popa O, Cocos R, et al. (2005) A deletion of a novel heat shock gene on the Y chromosome associated with azoospermia. Mol Hum Reprod 11: 295–298.
30. Dieterich K, Soto Rifo R, Karen Faure A, Hennebicq S, Amar BB, et al. (2007) Homozygous mutation of AURKC yields large-headed polyploid spermatozoa and causes male infertility. Nat Genet 39: 661–665.
31. Stranger BE, Forrest MS, Clark AG, Minichiello MJ, Deutsch S, et al. (2005) Genome-wide associations of gene expression variation in humans. PLoS Genet 1: e78. doi:10.1371/journal.pgen.0010078
32. Friedrich M, Grahnert A, Paasch U, Tannapfel A, Koch-Nolte F, et al. (2006) Expression of toxin-related human mono-ADP-ribosyltransferase 3 in human testes. Asian J Androl 8: 281–287.
33. Benjamini Y, Hochberg Y (1995) Controlling the false discovery rate: a practical and powerful approach to multiple testings. J R Statist Soc B 57: 289–300.
34. Livak KJ, Schmittgen TD (2001) Analysis of relative gene expression data using real-time quantitative PCR and the $2^{-\Delta\Delta CT}$ Method. Methods 25: 402–408.
35. Lewontin RC (1964) The interaction of selection and linkage. I. General considerations; heterotic models. Genetics 49: 49–67.
36. Hill WG, Robertson A (1968) Linkage disequilibrium in finite populations. Theor Appl Genet 38: 226–231.
37. Excoffier L, Slatkin M (1995) Maximum-likelihood estimation of molecular haplotype frequencies in a diploid population. Mol Biol Evol 12: 921–927.

Available online at www.sciencedirect.com
ScienceDirect
Gynecologic Oncology 109 (2008) 49–52
Gynecologic Oncology
www.elsevier.com/locate/ygyno

Conservative treatment of stage IA1 adenocarcinoma of the cervix during pregnancy

Tetsuro Yahata [a,*], Masahiro Numata [a], Katsunori Kashima [a], Masayuki Sekine [a], Kazuyuki Fujita [a], Takashi Yamamoto [b], Kenichi Tanaka [a]

[a] *Division of Obstetrics and Gynecology, Niigata University, Graduate School of Medical and Dental Sciences, 1-757 Asahimachi-dori, Chuo Ward, Niigata 951-8510, Japan*
[b] *Division of Cellular and Molecular Pathology, Niigata University, Graduate School of Medical and Dental Sciences, Niigata, Japan*

Received 17 October 2007
Available online 4 March 2008

Abstract

Objective The incidence of glandular neoplasms of the uterine cervix has been steadily increasing over the past 2 decades. These lesions tend to arise in women of childbearing age. Few reports have described the treatment of glandular neoplasms of the cervix in gravid women. This report describes the preliminary results of treating stage IA1 cervical adenocarcinoma by cervical conization during pregnancy.

Methods. All patients diagnosed to have FIGO stage IA1 cervical adenocarcinoma between 1990 and 2006 were reviewed and patients diagnosed during pregnancy were identified. Information was abstracted on the clinical data including the presence or absence of disease at the margins of conization, pregnancy outcome, and the follow-up.

Results. Sixteen patients with stage IA1 cervical adenocarcinoma were identified. Four out of the 16 patients were diagnosed during pregnancy. Four women ages 29–37 underwent KTP LASER conization and vaporization at 16 to 23 weeks' gestation. The histology showed that all of the tumors were endocervical type adenocarcinoma. None had lymph-vascular space invasion. All of these patients expressed a strong desire to continue their pregnancy. Two patients had positive conization margins for invasive cancer and underwent a second conization at 20 weeks' gestation and 5 weeks after delivery, respectively. No residual disease was identified in the second conization specimens. All patients delivered at term. One patient was treated with cervical conization alone and 3 patients were treated with an extended radical hysterectomy with pelvic lymph nodes dissection after delivery. No patient had residual invasive cancer in a subsequent surgical specimen. None of the patients had developed recurrent disease after a 2–13-year follow-up.

Conclusion. These preliminary data suggest that patients with FIGO stage IA1 cervical adenocarcinoma may be treated conservatively by cervical conization during pregnancy. Although a hysterectomy should be considered at the completion of childbearing, fertility sparing postpartum management could be an option for selected patients.

Keywords: Microinvasive adenocarcinoma; Cervical cancer; Stage IA1; Pregnancy; Conization

Introduction

The incidence of glandular neoplasms of the uterine cervix has been steadily increasing over the past 2 decades [1]. Because these lesions tend to arise in women of childbearing age, there is a particular need to understand whether they are amenable to conservative treatment. In the case of squamous lesions, cervical conization alone followed by careful observation is often preferred to hysterectomy in microinvasive cancer patients with a strong desire to preserve their fertility. Recently, emerging data support the conservative management of adenocarcinoma in situ (AIS) by cervical conization, provided the margins of the cone are clear [2–4]. Although some reports have suggested conization with a negative margin to also be acceptable as a final treatment

* Corresponding author. Fax: +81 25 227 0789.
E-mail address: yahatat@med.niigata-u.ac.jp (T. Yahata).

0090-8258/$ - see front matter © 2008 Elsevier Inc. All rights reserved.
doi:10.1016/j.ygyno.2008.01.016

Table 1
Clinical characteristics of women diagnosed with stage IA1 cervical adenocarcinoma during pregnancy

No.	Age	G/P	GA at Pap	Pap diagnosis	Diagnosis of biopsy	GA at conization	Diagnosis of conization	Grade	Depth Of invasion
1	29	1/1	–	–	Adenoca (undetermined invasion)	23 weeks	Microinvasive adenoca (endocervical type)	1	0.8 mm
2	34	3/0	9 weeks	CIN3	Microinvasive adenoca	19 weeks	Microinvasive adenoca (endocervical type)	1	0.7 mm
3	37	2/1	7 weeks	CIN1	Microinvasive squamous cell carcinoca	20 weeks	Microinvasive adenoca (endocervical type)	1	1.3 mm
4	37	1/1	8 weeks	adenoca	Adenoca (undetermined invasion)	16 weeks	Microinvasive adenoca (endocervical type)	1	2.0 mm

G/P: gravity/parity.
GA: gestational age.
Adenoca: adenocarcinoma

for stage IA1 adenocarcinoma like its squamous counterpart [5,6], much less is known about the management of adenocarcinoma because of its rarity.

Gravid women are rarely diagnosed with glandular neoplasms of the uterine cervix. Although there have been several reports regarding the management of AIS during pregnancy [7,8], a search of MEDLINE yielded no report on the management of microinvasive adenocarcinoma during pregnancy. The purpose of this study was to review the recent results of managing microinvasive adenocarcinoma of the cervix during pregnancy.

Materials and methods

Between 1990 and 2006, cases of FIGO stage IA1 cervical adenocarcinoma diagnosed at Niigata University Medical and Dental Hospital were reviewed and patients diagnosed during pregnancy were identified. Stage IA1 tumors were defined as buds of malignant cells arising from a gland with adenocarcinoma in situ in which stromal invasion was 3 mm or less in depth and 7 mm or less in diameter in the conization specimens. All cervical conizations were performed using a KTP LASER technique under lumbar anesthesia. The output power of KTP LASER was set at 10–15 W. A large dome-like contact conization was done with the additional vaporization of the surrounding tissue and the endocervix at an average depth of 1 mm. A cold knife was used to cut the cervical canal in order to avoid thermal artifacts at the endocervical margin on

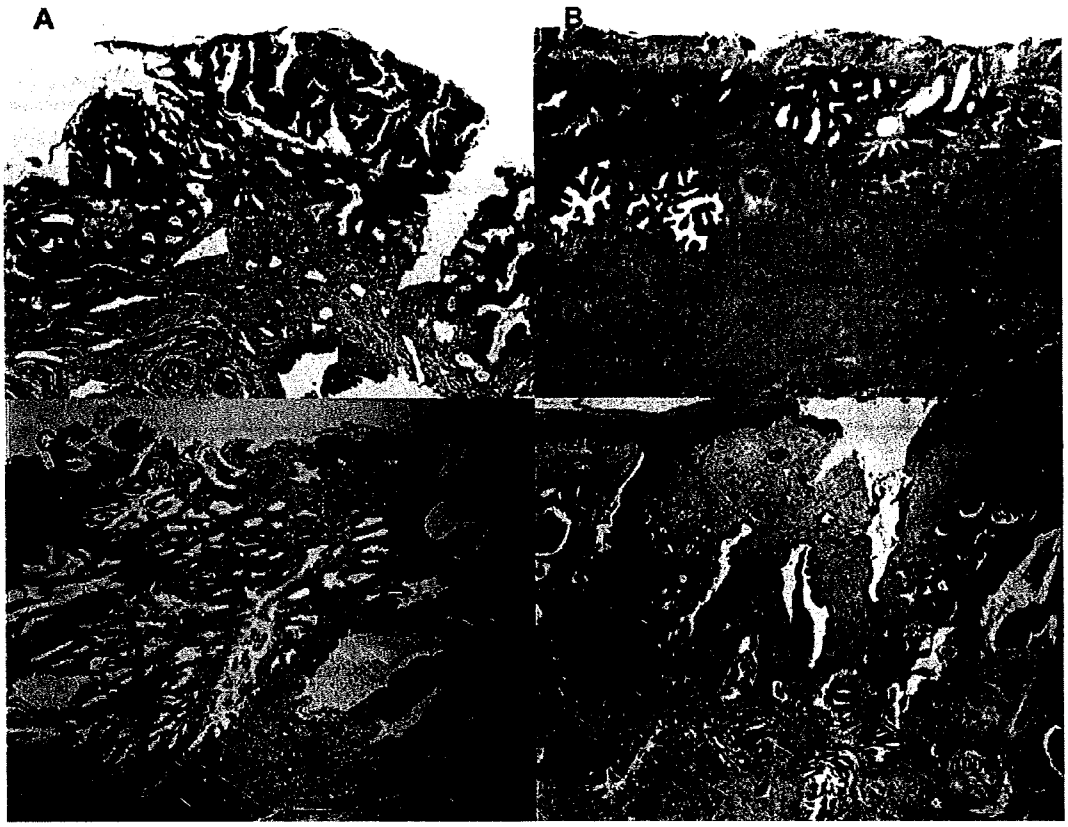

Fig. 1. Histopathology slides of conization specimen. A: Patient 1., B: Patient 2., C: Patient 3., D: Patient 4. The depth of invasion as measured from the surface epithelium was 0.8 mm, 0.7 mm, 1.3 mm, and 2.0 mm, respectively (Hematoxylin & Eosin stain, 40× original magnification).

Table 2
Outcomes of treatment and pregnancy

No.	Margin status of conization	Secondary surgery during pregnancy	Residual desease	Pap test after surgery	Mode of delivery (GA)	Postpartum treatment	Residual disease	Current status (months##)
1	Negative	None	NA	Negative	Vaginal (39 weeks)	AH, PLA	AIS	NED (155)
2	Positive	None	NA	AGC	Vaginal (38 weeks)	Conization	None	ND (34)
3	Negative	None	NA	Negative	C/S (37 weeks)#	AH, PLA#	AIS	NED (130)
4	Positive	Conization (20 weeks)	None	Negative	C/S (41 weeks)	AH, PLA	None	NED (24)

NA: not applicable.
AGC: atypical glandular cells.
GA: gestational age.
C/S: Cesarean section.
AH: abdominal hysterectomy (type II).
PLA: pelvic lymphadenectomy.
AIS: adenocarcinoma in situ.
NED: no evidence of disease.
#: C/S following the definitive surgery.
##: months after postpartum treatment.

the conization specimen. All patients were performed Shirodkar's cervical encerclage and received prophylactic tocolytic therapy.

Postconization surveillance consisted of a Pap smear every 8 weeks. The patients were informed that any abnormality would be evaluated by colposcopy, directed biopsies, and a repeat conization or hysterectomy if indicated. The data were retrospectively extracted from the patient's medical records and information was abstracted on clinical data including the presence or absence of disease at the margins of conization, pregnancy outcome, and follow-up.

Results

Sixteen patients with stage IA1 adenocarcinoma of the cervix were identified. Four out of the 16 patients were diagnosed during pregnancy (Table 1). The antecedent Pap smear tests occurred at 7 to 9 weeks' gestation. Diagnoses of subsequent biopsies were invasive adenocarcinoma in three patients (undetermined invasion in two patients) and squamous cell carcinoma in one patient. All of these patients underwent a cervical conization at 16 to 23 weeks' gestation. None of the procedures were complicated by excessive blood loss, premature labor, or miscarriage. The diagnosis of the conization was microinvasive adenocarcinoma with 0.7–2.0 mm of stromal invasion (Fig. 1). A histological analysis showed all of the tumors to be endocervical type adenocarcinomas. None had lymph-vascular space invasion. All these patients expressed a strong desire to continue their pregnancy.

Outcomes of treatment and pregnancy were summarized in Table 2. Two patients had positive cone margins for invasive cancer and underwent second conizations at 20 weeks' gestation and 5 weeks after delivery, respectively. No residual disease was identified in the second conization specimen. All of the patients delivered at term: including 2 vaginally and 2 by Cesarean delivery. Cesarean delivery was selected due to the patient's desire for a hysterectomy at the time of delivery in one patient and due to an arrest of labor for the other patient. One patient was treated with cervical conization (repeated conization) alone. She had normal Pap smear test and endocervical curettage findings during a follow-up of 34 months. Three patients were treated with extended radical hysterectomies with pelvic lymph nodes dissection after delivery. Although no patient had any residual invasive cancer in a subsequent surgical specimen, residual AIS was seen in two patients with negative cone margins. No lymph node metastasis was found. None of these patients have since developed recurrent disease during a 3–13-year follow-up.

Discussion

It is widely held that, in stage IA1 cervical squamous cell carcinoma with no lympho-vascular involvement, a cervical conization with negative margins is acceptable as a final treatment. However, the appropriate treatment of microinvasive cervical adenocarcinoma remains controversial because some authors have reported multifocal lesions high in the cervical canal which were missed even on cervical conization [5,9]. Given that the incidence of cervical adenocarcinoma is increasing and that disease is being diagnosed at an earlier stage and that it often occurs in young women, minimizing the morbidity associated with the treatment of very early lesions is now becoming increasingly important.

Smith et al. reviewed a total of 585 cases of stage IA1 adenocarcinoma and reported the incidence of positive lymph nodes was 1.5–1.6% (4/234–277) and the censored survival rate was 99.1% (5/585) [10]. They described no reported recurrences in 98 cases managed by cervical conization as a definitive surgery. These data support the hypothesis that stage IA1 adenocarcinoma can be treated in the same way as its squamous counterpart since it has an excellent prognosis. However 10% of the patients in their report received adjuvant radiation therapy or underwent a pelvic lymphadenectomy. Therefore, cervical conization alone for all patients with stage IA1 adenocarcinoma was not advocated.

The occurrence of carcinoma of the cervix during pregnancy is relatively rare with an incidence of approximately 1 per 1200 to 10,000 pregnancies [11]. Although gravid women are rarely diagnosed with glandular neoplasms of the uterine cervix, the increase in the number of patients with cervical adenocarcinoma in young women may represent an increased incidence of cervical adenocarcinoma during pregnancy. There have been several reports regarding the management of AIS during pregnancy [2–4], however no information on the management of microinvasive adenocarcinoma during pregnancy is available. In this hospital, 4

(25%) patients were diagnosed during pregnancy among the 16 patients with stage IA1 cervical adenocarcinoma. This report describes our preliminary experience in the management of these patients.

An accurate diagnosis of glandular lesions is more difficult than for squamous lesions, since the colposcopic features commonly associated with squamous lesions can be entirely absent and skip lesions are more common with glandular neoplasms. Therefore, cervical conization is more frequently required to confirm or rule out invasive adenocarcinoma in cases with an abnormal glandular cytopathology. To date 18 cases of AIS associated with pregnancy have been reported with detailed clinical information [7,8,12]. Eleven out of 18 cases underwent uncomplicated cervical conization at 11 to 16 weeks' gestation. Seven cases that did not undergo conization were in a relatively advanced gestational age (16 to 30 weeks of gestation) when conization was considered. Of those 7 patients treated postpartum, one had stage IB1 cervical adenocarcinoma. Therefore, the authors emphasize the need for urgent evaluation by conization when atypical glandular cells are detected on a Pap smear test during pregnancy. In this study all four patient underwent uncomplicated diagnostic conization at 16 to 23 weeks' gestation. Cervical conization during the second trimester of pregnancy could be performed safely and it may be necessary in order to make an accurate diagnosis and select the optimal treatment strategies for glandular lesions.

The margin status is important since it correlates with both residual and recurrent disease. Cervical conization during pregnancy often results in positive section margins and residual disease. Dunn et al. have reported a 46% (6/13) incidence of positive margins in pregnant women [13]. Consistent with their report 2 of the 4 patients had positive margins in this study. Both patients underwent a second conization, one during pregnancy and another during the postpartum period, with no residual disease. Even if the cone margin is positive, the patients with stage IA1 adenocarcinoma could be managed expectantly for the reminder of the pregnancy following a close follow-up by cytology and colposcopy. A second conization should therefore be considered depending on the gestational age when the residual disease is suspected.

Fertility sparing postpartum management is an option for selected patients. One patient with a positive cone margin expressed a strong desire to preserve her uterus. She thus underwent a second conization after a vaginal delivery. No residual disease was found and she has been disease free for 34 months. It is important to note that the benefits of preserving the uterus may increase the risk of recurrence and, therefore, a careful follow-up is required. Although fertility sparing postpartum management could be an option for selected patients, hysterectomy should be considered at the completion of childbearing. Only women who are willing to accept such additional risks may be candidates for fertility sparing surgery.

Three patients were treated with an extended radical hysterectomy with pelvic lymph nodes dissection after delivery. Although no patient had residual invasive cancer in a subsequent surgical specimens, residual AIS was seen in two patients with negative cone margins. The incidence of residual disease in patients with glandular lesions remains high despite the margin status. Goldstein and Mari have reported the incidence of residual disease to be 30% with negative cone margin and 44% in positive cone margin in patients with AIS [14]. It seems that the involved margins do not always result in treatment failure and clear margins do not guarantee the complete eradication of a lesion, especially in cases with glandular lesions. Therefore, definitive surgery should be considered at the completion of childbearing because of the high rate of residual disease.

This report described patients with stage IA1 cervical adenocarcinoma during pregnancy who were managed by cervical conization with a good perinatal outcome. The four patients in this report illustrate distinct management options. Although the recommendation for therapy should be individualized based on the gestational age at diagnosis and the patient's desire to bear a child, conservative treatment by cervical conization during pregnancy is considered to be an acceptable treatment modality for both the mother and fetus.

References

[1] Sasieni P, Adams J. Changing rates of adenocarcinoma and adenosquamous carcinoma of the cervix in England. Lancet 2001;357:1490–3.
[2] Soutter WP, Haidopoulos D, Gornall RJ, McIndoe GA, Fox J, Mason WP, et al. Is conservative treatment for adenocarcinoma in situ of the cervix safe? Bjog 2001;108:1184–9.
[3] Bryson P, Stulberg R, Shepherd L, McLelland K, Jeffrey J. Is electrosurgical loop excision with negative margins sufficient treatment for cervical ACIS? Gynecol Oncol 2004;93:465–8.
[4] Andersen ES, Nielsen K. Adenocarcinoma in situ of the cervix: a prospective study of conization as definitive treatment. Gynecol Oncol 2002;86:365–9.
[5] McHale MT, Le TD, Burger RA, Gu M, Rutgers JL, Monk BJ. Fertility sparing treatment for in situ and early invasive adenocarcinoma of the cervix. Obstet Gynecol 2001;98:726–31.
[6] Schorge JO, Lee KR, Sheets EE. Prospective management of stage IA(1) cervical adenocarcinoma by conization alone to preserve fertility: a preliminary report. Gynecol Oncol 2000;78:217–20.
[7] Lacour RA, Garner EI, Molpus KL, Ashfaq R, Schorge JO. Management of cervical adenocarcinoma in situ during pregnancy. Am J Obstet Gynecol 2005;192:1449–51.
[8] Griffin D, Manuck TA, Hoffman MS. Adenocarcinoma in situ of the cervix in pregnancy. Gynecol Oncol 2005;97:662–4.
[9] Bertrand M, Lickrish GM, Colgan TJ. The anatomic distribution of cervical adenocarcinoma in situ: implications for treatment. Am J Obstet Gynecol 1987;157:21–5.
[10] Smith HO, Qualls CR, Romero AA, Webb JC, Dorin MH, Padilla LA, et al. Is there a difference in survival for IA1 and IA2 adenocarcinoma of the uterine cervix? Gynecol Oncol 2002;85:229–41.
[11] Nguyen C, Montz FJ, Bristow RE. Management of stage I cervical cancer in pregnancy. Obstet Gynecol Surv 2000;55:633–43.
[12] Nagaishi M, Fujiwaki R, Hata K, Makihara K, Yamane Y, Miyazaki K. Adenocarcinoma in situ coexisting with carcinoma in situ of the cervix during pregnancy. Arch Gynecol Obstet 2004;270:116–8.
[13] Dunn TS, Ginsburg V, Wolf D. Loop-cone cerclage in pregnancy: a 5-year review. Gynecol Oncol 2003;90:577–80.
[14] Goldstein NS, Mani A. The status and distance of cone biopsy margins as a predictor of excision adequacy for endocervical adenocarcinoma in situ. Am J Clin Pathol 1998;109:727–32.

doi:10.1111/j.1447-0756.2008.00784.x J. Obstet. Gynaecol. Res. Vol. 34, No. 3: 408–412, June 2008

Adenocarcinoma arising from respiratory ciliated epithelium in benign cystic teratoma of the ovary: A case report with analyzes of the CT, MRI, and pathological findings

Tetsuro Yahata[1], Takashi Kawasaki[2], Takehiro Serikawa[1], Mina Suzuki[1] and Kenichi Tanaka[1]

[1]*Department of Obstetrics & Gynecology, and* [2]*Division of Cellular and Molecular Pathology, Department of Cellular Function, Niigata University School of Medicine, Niigata, Japan*

Abstract

The malignant transformation of mature cystic teratoma is rare, thus occurring in only 1–2% of all cases. The most common malignancy arising in mature cystic teratoma is squamous cell carcinoma. Adenocarcinoma occurs with less frequency. We herein present a patient with an ovarian mature cystic teratoma who demonstrated a malignant transformation to well-differentiated adenocarcinoma. Malignant transformation was diagnosed preoperatively by contrast enhanced computed tomography (CT) and magnetic resonance imaging (MRI). Microscopically and immunohistochemically, the adenocarcinoma was considered to have arisen from the ciliated respiratory epithelium. After a 28-month of follow-up period, she remains free of the disease. This is the third reported case of adenocarcinoma arising in the respiratory epithelium of an ovarian mature cystic teratoma. Contrast enhanced CT and MRI are useful for making a preoperative diagnosis and an immunohistochemical study is helpful for defining its origin.

Key words: adenocarcinoma, CT, malignant transformation, mature cystic teratoma of the ovary, MRI.

Introduction

Mature cystic teratoma is the most common of all ovarian neoplasms. Malignant transformation of ovarian mature cystic teratoma occurs in from 1 to 2% of all cases.[1,2] Patients found to have malignant transformation are likely to be post-menopausal. Squamous cell carcinoma shows the highest incidence with 75–85% of such malignant transformations found in the ovarian mature cystic teratoma. Adenocarcinoma associated with mature cystic teratoma is extremely rare. To our knowledge, only two previous cases of adenocarcinoma arising in the respiratory epithelium of an ovarian mature cystic teratoma have so far been reported in the English literature.[3,4] We herein present a case of adenocarcinoma arising from the ciliated respiratory epithelium, in which computed tomography (CT) and magnetic resonance imaging (MRI) were useful for making an accurate preoperative diagnosis of malignant transformation and the pathologic findings were helpful for defining its origin.

Case Report

A 79-year-old woman, gravida 5, para 2, presented at our service with the chief complaint of a slight increase in her abdominal girth over the previous 3 months. She

Received: July 5 2007.
Accepted: September 6 2007.
Reprint request to: Dr Tetsuro Yahata, Department of Obstetrics & Gynecology, Niigata University School of Medicine, 1-757 Asahimachi-dori, Niigata 951-8510, Japan. Email: address: yahatat@med.niigata-u.ac.jp

had medical histories of hypertension and articular rheumatism. Her surgical, gynecologic, and family histories were all unremarkable. The patient reported that 3 years prior to current admission she had been diagnosed by CT and MRI to have an ovarian tumor measuring 7-cm in size, which was suspected to be a dermoid cyst. Thereafter, she had been scheduled to undergo repeat examination but did not show up and thus was lost to the follow-up.

On physical examination, a mobile pelvic mass measuring approximately 12 cm in size was palpated. Her external genitalia and vagina were normal. The cervix and uterine body were also normal. Laboratory tests including CBC, electrolytes and liver function tests were all within the normal limits. Elevated levels of CA19-9: 599 U/mL (normal limit <37) and CA125: 70 U/mL (normal limit <32) were found. Malignant transformation in ovarian mature cystic teratoma was highly suspected by preoperative CT and MRI of the abdomen and pelvis using intravenous contrast (detailed findings are described later), and a laparotomy was thus performed after obtaining the patient's informed consent. During the surgical procedure, a 12 cm cystic left adnexal mass was found. Both pelvic and peritoneal washing specimens were obtained and revealed no malignant cells. The contralateral ovary demonstrated normal findings. The uterus, other pelvic structures and the upper abdomen all showed a normal appearance. A left salpingo-oophorectomy was performed. The capsule of the tumor was not disrupted during the surgical procedure. An intraoperative examination of frozen sections of the left adnexal mass revealed a focus of adenocarcinoma arising from a mature cystic teratoma of the left ovary. Therefore, a modified staging procedure was performed including a total hysterectomy, and a right salpingo-oophorectomy. Biopsies of the lymphnodes and omentum were not performed because palpation and an inspection of the abdominal and pelvic lymphnodes and omentum indicated neither swelling nor dissemination. The final pathological diagnosis was confirmed to be a focus of well-differentiated adenocarcinoma within the left mature cystic teratoma. All other specimens were benign, thus resulting in a completely resected FigO stage IA, grade 1 adenocarcinoma of the left ovary. The patient's postoperative course was satisfactory and the CA19-9 and CA125 levels returned to normal within 3 weeks of the operation. The patient received no further treatment and remains free of disease at 28 months after the operation.

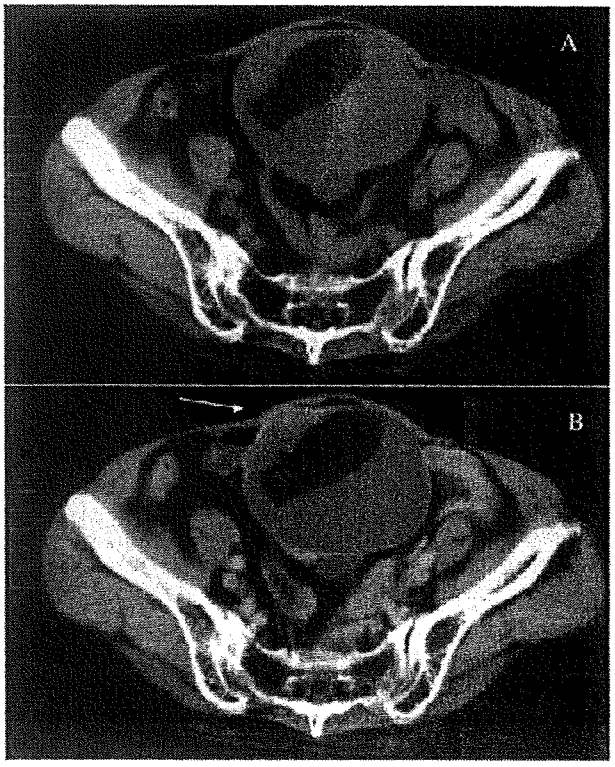

Figure 1 Horizontal CT scans. A. Without contrast the 10 cm-sized regularly margined tumor with cystic component and floating fat component part were shown. B. After iohexol administration the solid part (white arrow) in the right side of the tumor wall becomes distinctively hyperdense.

CT and MRI Findings

CT scans of the chest, abdomen, and pelvis and MRI of the pelvis with intravenous contrast were performed. They revealed a regularly marginated adnexal mass measuring $10 \times 10 \times 8$ cm in size in the pelvis. The tumor was composed of cystic, solid areas, and fatty components. The fatty components, fat density in CT and high-intensity (T1-weighted), intermediate-intensity (T2-weighted) in MRI, were found to be floating in the cystic part of the tumor. The solid part of the tumor, which measured 2 cm in diameter, was observed on the right side of the tumor wall. After the administration of contrast medium, the solid part was enhanced both in CT and MRI (Figs 1,2). An intramural myoma that measured 5 cm in its largest diameter was seen in the posterior wall of the uterus. The upper abdomen and chest were within the normal limits. The contralateral ovary was not detected by either CT or MRI.

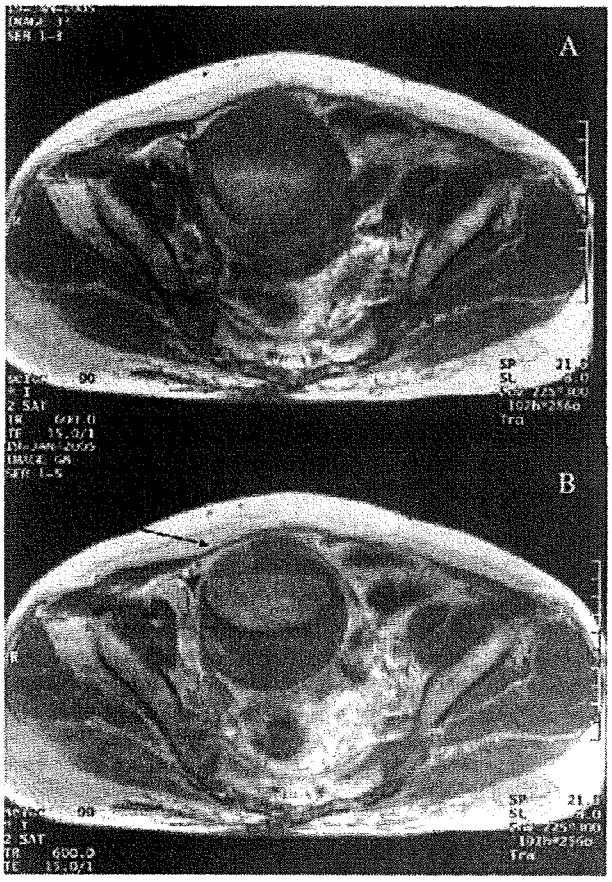

Figure 2 Horizontal T1 weighted MR images. Without contrast the solid part (*black arrow*) has a hypointense signal. After gadolinium administration the solid part becomes distinctively hyperintense.

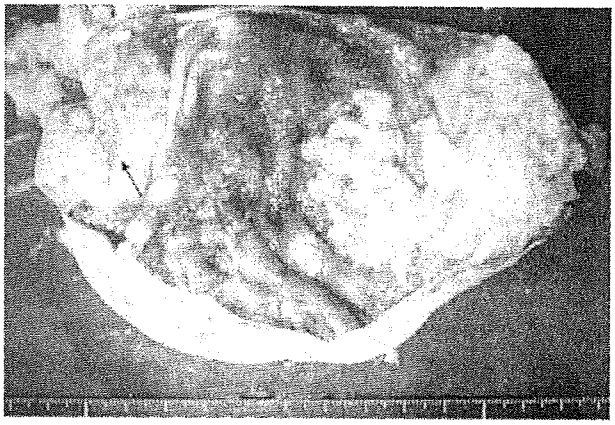

Figure 3 Gross appearance of tumor on cut section. The 2 cm-sized tan-yellowish solid part (black arrow) is demonstrated.

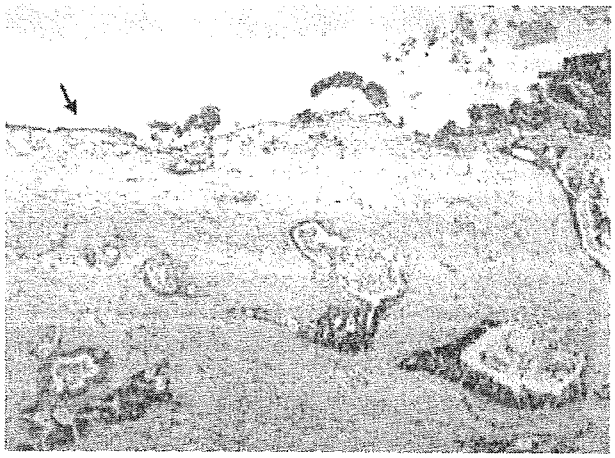

Figure 4 Microscopic findings of the tumor (HE × 200). The left part is the ciliated columnar epithelium like the mucosa of the respiratory tract (black arrow). The transition from ciliated columnar epithelium to well-differentiated adenocarcinoma (white arrow) was noted.

Pathological Findings

The surgical specimen of the left ovarian tumor consisted of a 10 × 10 × 8 cm cystic mass containing hair, fat, and keratinaceous debris. The external surface was not disrupted. The cyst lining was slightly thickened and 2 cm-sized tan-yellowish solid part was seen corresponding to that enhanced by CT and MRI (Fig. 3). The histologic sections from the cyst wall disclosed a mature cystic teratoma that contained mature tissue of skin, small mucinous glands, adipose tissue, and respiratory ciliated columnar epithelium. Sections from the area of the solid part showed a well-differentiated adenocarcinoma arising from the mature cystic teratoma. The transition from ciliated columnar epithelium to well-differentiated adenocarcinoma was noted (Fig. 4). The adenocarcinoma cells also had cilia on their surface. The nuclei of the tumor cells were enlarged and irregularly shaped and contained coarse chromatin and large nucleoli. No lymphovascular space invasion was observed. In addition, the ovarian surface was not involved with the tumor.

The ciliated epithelium was negative for Alcian blue staining, positive for cytokeratin-7 (CK7) and negative for cytokeratin-20 (CK20) using immunoperoxidase stainings techniques. The tumor cells were also negative for Alcian blue stains, positive for CK7 and marginally positive for CK20 (Fig. 5). Both the ciliated epithelium and tumor cells were positive for CA19-9 and negative for estrogen receptor (ER).

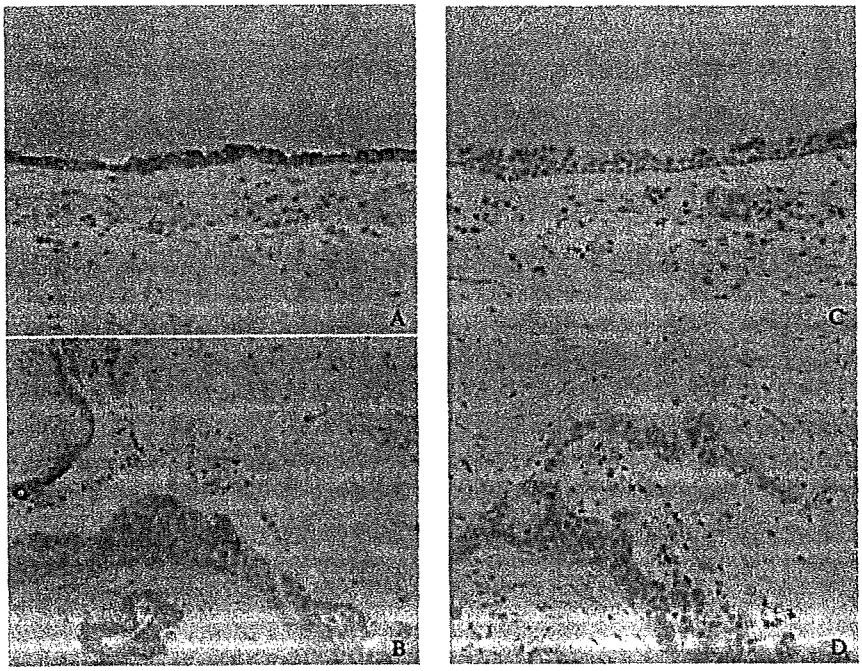

Figure 5 Immunohistochemical findings (x200). A. The benign columnar epithelium was positive for CK-7. B. The adenocarcinoma was positive for CK-7. C. The benign columnar epithelium was negative for CK-20. D. The adenocarcinoma was marginally positive for CK-20.

Morphologically and immunohistochemically, the origin of the tumor defined respiratory epithelium. Leiomyoma was seen in the uterus. The contralateral ovary showed normal pathologic findings.

Discussion

Mature cystic teratoma is the most common ovarian teratoma as well as the most common ovarian germ cell neoplasm. These tumors consist of maturely differentiated derivatives of all three germ cell layers, with the ectodermal layer being most prominent. Malignant transformation of the mature cystic ovarian teratoma occur in from 1 to 2% of all cases.[1,2] Malignant transformation typically occurs in post-menopausal women, although a diagnosis in pre-menopausal women is not extraordinary. It occurs between the ages of 30 and 70 years and the most common malignancy is squamous cell carcinoma which represent 75% of the malignant transformation. There have been several reports of adenocarcinoma arising in mature cystic teratoma. Peterson reviewed 15 adenocarcinomas and found that the histologic origins were from mammary, salivary, sebaceous, and thyroid gland epithelia, but not from the respiratory epithelium.[5] So far, only two reports of case with respiratory epithelium origin have been reported.[3,4]

CT and MRI are useful for making a preoperative diagnosis as with other ovarian tumors.[6] The presence of fat, fluid (with fat-fluid level), and subtle calcification are the most characteristic radiologic findings of mature cystic teratoma. However fat-fluid levels and calcification could be seen in the malignant transformation of teratoma.[6] As a result, benign and malignant teratomas cannot be consistently distinguished by those findings on CT and MRI. Nevertheless, the imaging characteristics of our case are suggestive of the presence of malignant transformation. Both CT and MRI facilitated the diagnosis of the malignant transformation of mature cystic teratoma due to enhanced images of the solid part with characteristic findings for mature teratoma. The enhanced solid part corresponded to the extent of adenocarcinoma in macro- and microscopic sections.

Tumor markers have also been useful for the preoperative diagnosis of malignant transformation of mature teratoma. Accordingly, 67% of the patients with a malignant transformation to squamous cell carcinoma have been reported to have elevated serum SCC antigen.[7] In the case of adenocarcinoma, elevated levels of CEA, CA19-9, CA125, CA72-4, CA15-3, and SLX have been reported.[2,3] In most reported cases, the serum CEA is elevated ranging from 5 to 70.6 mg/dL[3] In our case, the serum CA19-9 level was considerably

higher (599 U/mL) in comparison to the mean serum CA19-9 level (79.4 U/mL) in patients with benign mature cystic teratoma.[8] As a result, these tumor markers might be useful for the preoperative diagnosis of malignant transformation to adenocarcinoma.

The definition of the adenocarcinoma origin in the present case is primarily based on the microscopic appearance. The adenocarcinoma lesion appeared to be continuous with the teratomatous ciliated columnar epithelium. This suggested that the lesion originated in the ciliated epithelium such as the respiratory airway and the Fallopian tube. The utility of cytokeratin immunostaining to determine the origin of adenocarcinoma has been reported by several authors.[2,9] Adenocarcinomas arising from the gastrointestinal tract are generally negative for CK7. In contrast, adenocarcinomas of the lung, pancreas, breast, and female genital tract are normally positive for CK7. Although immunostaining for CK7 and CK20 is considered to be helpful for distinguishing the gastrointestinal tract from other origins, they are not able to distinguish between adenocarcinomas of the lung and the female genital tract. Estrogen receptor (ER) is expressed in the estrogen target organs including female genital tracts. Immunohistochemical staining of ER has been reported to be positive for ciliated and secretory cells of the Fallopian tube.[10] Both the ciliated epithelium and adenocarcinoma were negative for ER indicating they were not the female genital tract origin. As a result, in our case, the adenocarcinoma was considered to originate from the respiratory epithelium since they arose from CK7 positive/CK20 negative/ER negative ciliated epithelium. It was also reported that CA19-9 was immunohistochemically demonstrated in the bronchial glands and bronchial mucosa of mature cystic teratoma.[8] The results of positive CA19-9 staining furthermore suggests the origin of adenocarcinoma in present case is respiratory epithelium.

Although teratomas with malignant transformation have a more aggressive clinical course than teratomas as whole, better prognosis has been reported when the malignant element is a squamous cell carcinoma confined to the ovary and is excised without any spillage of the contents.[2,6] Although our experience with these tumors is limited, it appears that this type of neoplasm may not be as dismal as previously believed, especially if there is no evidence of metastasis at presentation. In our case, the treatment options were carefully discussed with the patient and adjuvant therapy was withheld because the disease was limited to within the left ovary. To our knowledge, the present case is the third presentation in the English literature of adenocarcinoma of respiratory epithelial origin arising in mature cystic teratoma.

References

1. Ueda G, Fujita M, Ogawa H *et al.* Adenocarcinoma in a benign cystic teratoma of the ovary: report of a case with a long survival period. *Gynecol Oncol* 1993; **48**: 259–263.
2. Kushima M. Adenocarcinoma arising from mature cystic teratoma of the ovary. *Pathol Int* 2004; **54**: 139–143.
3. Sumi T, Ishiko O, Maeda K *et al.* Adenocarcinoma arising from respiratory ciliated epithelium in mature ovarian cystic teratoma. *Arch Gynecol Obstet* 2002; **267**: 107–109.
4. Cobellis L, Schurfeld K, Ignacchiti E *et al.* An ovarian mucinous adenocarcinoma arising from mature cystic teratoma associated with respiratory type tissue: a case report. *Tumori* 2004; **90**: 521–524.
5. Peterson WF. Malignant degeneration of benign cystic teratomas of the ovary; acollective review of the literature. *Obstet Gynecol Surv* 1957; **12**: 793–830.
6. Wang LJ, Chu SH, Ng KF *et al.* Adenocarcinomas arising from primary retroperitoneal mature teratomas: CT and MR imaging. *Eur Radiol* 2002; **12**: 1546–1549.
7. Tseng CJ, Chou HH, Huang KG *et al.* Squamous cell carcinoma arising in mature cystic teratoma of the ovary. *Gynecol Oncol* 1996; **63**: 364–370.
8. Ito K. CA19-9 in mature cystic teratoma. *Tohoku J Exp Med* 1994; **172**: 133–138.
9. Lagendijk JH, Mullink H, van Diest PJ *et al.* Immunohistochemical differentiation between primary adenocarcinomas of the ovary and ovarian metastases of colonic and breast origin. Comparison between a statistical and an intuitive approach. *J Clin Pathol* 1999; **52**: 283–290.
10. Comer MT, Leese HJ, Southgate J. Induction of a differentiated ciliated cell phenotype in primary cultures of Fallopian tube epithelium. *Hum Reprod* 1998; **13**: 3114–3120.